

Single-cell imaging of intracellular Ca^{2+} and phospholipase C activity reveals that RGS 2, 3 and 4 differentially regulate signaling via the $\text{G}\alpha_{q/11}$ -linked muscarinic M_3 receptor

Stephen C. Tovey and Gary B. Willars[#]

Department of Cell Physiology and Pharmacology, University of Leicester, Leicester, UK.

- a) **Running title:** RGS mediated inhibition of muscarinic M₃ receptor signaling
- b) **Correspondence:** Dr. Gary. B. Willars, Department of Cell Physiology and Pharmacology, Medical Sciences Building, University of Leicester, University Road, LE1 9HN, United Kingdom. Tel: +44 116 2523094. Fax: +44 116 2525045. E-mail: gbw2@le.ac.uk.

c) Number of text pages:	37
Number of tables	1
Number of figures	9
Number of references	38
Number of words in the abstract	223
Number of words in the Introduction	708
Number of words in the Discussion	1479

d) Non-standard abbreviations:

[³ H]-InsP _x	[³ H] mono- and polyphosphates of inositol
[³ H]-NMS	1-[<i>N</i> -methyl- ³ H]scopolamine methyl chloride
CA-Gα _q	constitutively active Gα _q (Q209L)
[Ca ²⁺] _i	intracellular Ca ²⁺ concentration
DH	dbl homology
DEP	dishelved, Egl-10, pleckstrin
eGFP	enhanced green fluorescent protein
eGFP-PH _{PLCδ1}	eGFP coupled to the PH domain of PLC _{δ1}
eGFP-PKCγC1 ₂	eGFP coupled to the diacylglycerol binding domain of the C1 ₂ region of PKCγ
GAP	GTPase activating protein
GGL	G-protein γ-like
GnRH	gonadotropin-releasing hormone
GPCR	G-protein coupled receptor
HEK	human embryonic kidney
HEK293/WT	wild-type HEK293 cells
HEK293/M ₃	HEK293 cells expressing recombinant human muscarinic M ₃ receptors
HEK293/RGS2 _{myc}	HEK293 cells expressing recombinant RGS2 _{myc}
HEK293/RGS3 _{myc}	HEK293 cells expressing recombinant RGS3 _{myc}
HEK293/RGS4 _{myc}	HEK293 cells expressing recombinant RGS4 _{myc}
Ins(1,4,5)P ₃	inositol (1,4,5) trisphosphate
KHB	Krebs' HEPES buffer
PH	pleckstrin homology
PLC	phospholipase C
RGS	regulator(s) of G-protein signaling

Abstract

Using single cell, real-time imaging, this study compared the impact of members of the B/R4 subfamily of the regulators of G-protein signaling (RGS) (RGS2, 3 and 4) on receptor-mediated $\text{Ins}(1,4,5)\text{P}_3$, diacylglycerol and Ca^{2+} signaling. In HEK293 cells expressing recombinant $\text{G}\alpha_{q/11}$ -coupled muscarinic M_3 receptors, transient co-expression of RGS proteins with fluorescently-tagged biosensors for either $\text{Ins}(1,4,5)\text{P}_3$ or diacylglycerol demonstrated that RGS2 and 3 inhibited receptor-mediated events. Although gross indices of signaling were unaffected by RGS4, it slowed the rate of increase in $\text{Ins}(1,4,5)\text{P}_3$ levels. At equivalent levels of expression, *myc*-tagged RGS proteins showed inhibitory activity in the order $\text{RGS3} \geq \text{RGS2} > \text{RGS4}$. In HEK293 cells, stable expression of *myc*-tagged RGS2, 3 or 4 at equivalent levels also inhibited phosphoinositide and Ca^{2+} signaling by endogenously expressed muscarinic M_3 receptors in the order $\text{RGS3} \geq \text{RGS2} > \text{RGS4}$. In these cells, either RGS2 or 3 reduced receptor-mediated inositol phosphate generation in cell populations and reduced both the magnitude and kinetics (rise-time) of single cell Ca^{2+} signals. Furthermore, at low levels of receptor activation, oscillatory Ca^{2+} signals were dampened or abolished whilst at higher levels, RGS2 and 3 promoted the conversion of more stable Ca^{2+} elevations into oscillatory signals. Despite little or no effect on responses to maximal receptor activation, RGS4 produced effects on the magnitude, kinetics and oscillatory behaviour of Ca^{2+} signaling at sub-maximal levels that were consistent with those of RGS2 and 3.

Introduction

The family of regulators of G-protein signaling (RGS) negatively regulate signaling by G-protein coupled receptors by binding to activated G α -subunits and acting as either GTPase activating proteins (GAPs) or effector antagonists (Hepler, 1999; Ross and Wilkie, 2000; Hollinger and Hepler, 2002). More than 30 distinct proteins are now known to exist that contain an RGS or RGS-like domain. This is an approximately 120 amino acid region through which these proteins can increase the intrinsic GTPase activity of GTP bound G α subunits. Interestingly, many RGS proteins contain other recognisable protein binding domains, such as the GGL (G-protein γ -like) (RGS6, 7, 9, 11) (Snow et al., 1998a) that confers binding to the G-protein subunit G β 5, PDZ (RGS12, PDZ-RhoGEF) (Hollinger and Hepler, 2002; Snow et al., 1998b), DEP (dishelved, Egl-10, pleckstrin) (RGS6, 7, 9, 11) (Snow et al., 1998a), DH (dbl homology) and PH (pleckstrin homology) domains (p115RhoGEF, PDZ-RhoGEF) (reviewed in Hollinger and Hepler, 2002). These domains may be involved in determining cellular localization, RGS specificity towards G α subunits and they may also confer signaling roles distinct from inhibition of G α -subunits (Hollinger and Hepler, 2002).

RGS and RGS-like proteins have been classified into sub-families based on the alignment of the RGS domain amino acid sequences (Ross and Wilkie, 2000; Zheng et al., 1999). According to this scheme, RGS2, 3 and 4 each belong to the B/R4 RGS sub-family of which RGS4 is considered the prototypical member. With the exception of RGS3, the B/R4 sub-family are small proteins (20-30kDa) that contain an N-terminal cationic amphipathic α helix that, at least for RGS4, is responsible for membrane attachment. Although RGS3 also contains an amphipathic α helix adjacent to its RGS domain, it is a relatively large (~70kDa) protein with an N-terminal region three times larger than the RGS domain. The function of this N-terminal region is, however, poorly understood (Castro-Fernandez and Conn, 2002).

RGS3 has previously been shown to inhibit signalling by several receptors, for example the $G\alpha_{q/11}$ -coupled gonadotropin-releasing hormone (GnRH) receptor (Castro-Fernandez and Conn, 2002; Neill et al., 1997). RGS4 has previously been shown to inhibit signalling by both $G\alpha_i$ - and $G\alpha_{q/11}$ -coupled receptors, for example the muscarinic M_2 and M_3 receptors respectively (Doupnik et al., 1997; Rumenapp et al 2001). In contrast, RGS2 lacks GAP activity towards $G\alpha_i$, at least *in vitro*, but is 5-10 fold more potent than RGS4 in blocking $G\alpha_q$ -mediated activation of phospholipase $C\beta$ (Heximer et al., 1997).

Many previous studies to assess the impact of RGS protein expression on the function of $G\alpha_{q/11}$ -coupled receptors have relied upon transient over-expression of RGS proteins and analysis of their affects in population based assays (such as total inositol phosphate accumulation) (Anger et al., 2004). Recently the advent of novel biosensors to detect the generation of either inositol 1,4,5 trisphosphate ($Ins(1,4,5)P_3$) (eGFP-PH_{PLC δ 1}) or diacylglycerol (eGFP-PKC γ C1₂) has allowed examination of phospholipase C (PLC) activity at the single cell level (Stauffer et al., 1998; Nash et al., 2001; Oancea et al., 1998; Oancea and Meyer, 1998). In particular, $Ins(1,4,5)P_3$ and diacylglycerol production can be determined at the single-cell level in real-time and at a spatial resolution previously unimaginable (Nahorski et al, 2003). The eGFP-PH_{PLC δ 1} construct represents a fusion protein of eGFP (enhanced green fluorescent protein) with the pleckstrin-homology domain of PLC δ 1. At rest eGFP-PH_{PLC δ 1} is localised to the plasma membrane, as it binds with high affinity and selectivity to phosphatidylinositol 4,5-bisphosphate ($PtdIns(4,5)P_2$) (Stauffer et al., 1998; Nash et al., 2001), but upon agonist stimulation it becomes cytosolic as $Ins(1,4,5)P_3$ is produced and binds to it with high affinity, thereby displacing it from the membrane (Nash et al., 2001). The eGFP-PKC γ C1₂ construct represents eGFP coupled to the diacylglycerol binding domain of the C1₂ region of PKC γ . Under resting conditions it has a cytosolic

localisation, but upon agonist stimulation and diacylglycerol production it is recruited to the plasma membrane (Oancea et al., 1998; Oancea and Meyer, 1998).

In the present study, we show for the first time that novel protein based biosensors to detect Ins(1,4,5)P₃ and diacylglycerol production can be used to examine how RGS proteins differentially regulate G $\alpha_{q/11}$ -mediated signaling via the muscarinic M₃ receptor at the single cell level. Further to this, we also show how RGS proteins differentially influence the pattern and kinetics of Ca²⁺ signaling at the single cell level.

Materials and Methods

Materials. Cell culture plastic-ware was from NUNC (Roskilde, Denmark) and cell culture reagents from Invitrogen (Paisley, U.K.). *myo*-[³H]-Inositol was from Amershambiosciences (Little Chalfont, Bucks., U.K.). Unless stated, other reagents were supplied by either Sigma Aldrich (Poole, U.K.), Fisher Scientific (Loughborough, U.K.), Merck (Darmstadt, Germany) or BDH Laboratory Supplies (Poole, U.K.).

Original RGS DNA constructs - Plasmids containing full-length constructs encoding human RGS2 (L13463), human RGS3 (U27655) and rat RGS4 (U27767) were gifts from Dr. Craig Doupnik (University of South Florida college of medicine, Tampa, FL, USA). The plasmids for RGS2 and RGS3 in the mammalian expression vector pRcCMV (Invitrogen, Paisley, UK) were originally from Dr. Kirk Druey and Dr. John Kehrl (National Institute of Health, Bethesda, MD, USA), whilst the plasmid for RGS4 in the mammalian expression vector pcDNA3.1 (Invitrogen, Paisley, UK) originated from Dr. Henry Lester (California Institute of Technology, Pasadena, CA, USA). The plasmid containing a constitutively active G α_q mutant (Q209L) (CA-G α_q) was a gift from Dr. Scott Heximer (University of Washington, St. Louis, MO, USA) and originated from Dr. John Hepler (Emory University, Atlanta, GA, USA). The vectors for the Ins(1,4,5)P₃ (eGFP-PH_{PLC δ 1}) and diacylglycerol (eGFP-PKC γ C1₂) biosensors were provided by Professor T. Meyer (Stamford University, CA, USA).

Generation of myc tagged constructs - RGS 2, 3 and 4 were PCR amplified from their original vectors to incorporate KpnI and XhoI restriction sites. The resulting PCR fragments were then column purified (Qiagen, Crawley, UK) and sub-cloned into pcDNA3.1/*myc*-His (Invitrogen, Paisley, UK). Expression of these constructs results in the generation of C-terminal *myc*-epitope tagged RGS proteins.

Establishing stable muscarinic M₃ expression in HEK293 cells - The generation of HEK293 cells stably expressing the muscarinic M₃ receptor was achieved using a standard calcium phosphate method. Wild type HEK293 cells (HEK293/WT) were transfected with the DNA encoding the human muscarinic M₃ receptor that had been cloned (BamH1/EcoR1) into the plasmid pcDNA3 (Invitrogen, Paisley, UK). Cells were selected with Genetecin (G-418; 500µg/ml) and clones expanded from single foci. Muscarinic receptor expression was determined by the binding of the muscarinic receptor antagonist 1-[*N*-methyl-³H]scopolamine methyl chloride ([³H]-NMS) exactly as described elsewhere (Willars et al., 1998) and a single clone selected for further study. These cells (HEK293/M₃ cells) express approximately 1.7pmol receptor per mg protein compared with approximately 40fmol muscarinic receptor per mg protein in HEK293/WT cells.

Cell culture and transfection - Both HEK293/M₃ and HEK293/WT cells were cultured in MEM alpha medium with Glutamax-1 and Earles' salts, supplemented with non-essential amino acids (1%), foetal calf serum (10%) and Gentamycin (50µg ml⁻¹). Cells were maintained in a humidified atmosphere (95% O₂:5% CO₂; 37°C) with the culture media replaced every third day and the cells passaged when they reached ~80% confluence. For single cell imaging, cells were plated onto 25mm borosilicate glass coverslips coated with 0.01% poly-D-lysine (Sigma, Poole, UK). After two days in culture, cells were transfected with the relevant DNA using Genejuice (Merck Bioscience, Nottingham, UK) at a ratio of 3:1 (Genejuice:DNA) according to the manufacturer's guidelines. Cells were used for imaging experiments 48h post-transfection.

Establishing stable RGSmyc expression in HEK293 cells - Stable RGSmyc expressing cell lines were made according to established protocols (Willars et al., 1998). Briefly, HEK293/WT cells were grown to ~50% confluence on 100mm cell culture dishes. Cells were then transfected with 3µg RGSmyc DNA using Genejuice as described above. After

48h, transfected cells were selected using G-418 (500 μ g/ml). Cells on transfected plates were allowed to grow until all cells on a control plate of untransfected cells had died. Transfected cells were then serially diluted and seeded into 96-well plates. Single colonies originating from individual cells were then selected and expanded for screening by Western blotting with an anti-*myc* antibody (New England Biolabs, Hitchin, UK). The stable expression of RGS*myc* proteins in selected clones was then confirmed throughout the experimental period using Western blotting.

Western blotting of RGSmyc proteins - Cells grown in 24- or 6-well plates were solubilized (10mM Tris, 10mM EDTA, 500mM NaCl, 1% Igepal CA630, 0.1% SDS, 0.5% deoxycholate, 1mM phenylmethylsulfonyl fluoride, 100 μ g ml⁻¹ iodoacetamide, and 100 μ g ml⁻¹ benzamidine, pH 7.4) and proteins (~30 μ g/lane) separated by SDS-PAGE using 8-12% running gels. Proteins were transferred onto nitrocellulose membranes, which were then blocked for 1h in 5% (w/v) skimmed milk powder in TTBS (137mM NaCl, 20mM Tris, pH 8.0, 0.05% Tween-20; pH 8.0) and incubated overnight at 4°C with primary antibody against the *myc* epitope (New England Biolabs, Hitchin, UK) at 1:1000 in 3% bovine serum albumin (BSA) in TTBS. Blots were then washed 3 times (10min each) in TTBS and incubated for 1h with an anti-rabbit HRP conjugated secondary antibody (Sigma, Poole, UK; 1:3000 in blocking buffer). After three further washes in TTBS (10min each) the blots were exposed to ECL Plus detection reagents (Amershambiosciences, Chalfont, UK) according to the manufacturer's guidelines and bands visualised using Hyperfilm (Amershambiosciences, Chalfont, UK).

Immunostaining of RGSmyc proteins - Cells were plated onto 22mm diameter glass coverslips and allowed to adhere for 48h prior to transfection. Immunostaining was carried out as previously described (Tovey et al., 2001). Briefly, cells were washed with phosphate buffered saline (PBS) and then immediately fixed for 30min in 4% paraformaldehyde in PBS.

After fixation, cells were permeabilised in PBS with 0.2% Triton-X100 (10min) and thereafter non-specific sites blocked by a 45min incubation with PBS containing 3% BSA and 0.2% Triton-X100. Cells were then incubated overnight at 4°C in primary antibody (anti-*myc*, 1:100 in PBS with 3% BSA). The following day cells were washed three times in PBS (10min) and then incubated for 1h with an anti-rabbit FITC conjugated secondary antibody (Vector Labs, Peterborough, UK; 1:250 in PBS with 10% goat serum). After three further washes (10min) in PBS, coverslips were mounted onto microscope slides using Vectorshield Fluorescence Preservative (Vector Labs, Peterborough, UK). FITC labelling was then visualised using an Olympus Fluoview confocal microscope.

Confocal imaging of eGFP-tagged biosensors and intracellular Ca^{2+} signals - Cells were transfected with eGFP-tagged biosensor DNA with or without RGS/RGSmyc DNA 48h prior to imaging as described above. Typically, an individual well of a 6-well multi-dish was transfected with 0.5µg of biosensor DNA alone, or co-transfected with 0.5µg of biosensor DNA and an excess of RGS/RGSmyc DNA (1.5µg) in order to ensure that all cells transfected with biosensor were co-transfected with RGS/RGSmyc DNA. Prior to imaging, the culture medium was replaced with a Krebs'-HEPES buffer (KHB) (composition (mM, unless otherwise stated): HEPES 10; NaHCO₃ 4.2; D-glucose 11.7; MgSO₄·7H₂O 1.18; KH₂PO₄ 1.18; KCl 4.69; NaCl 118; CaCl₂·2H₂O 1.29; 0.01% w/v BSA, pH 7.4). Cells were then mounted onto the stage of an Olympus IX50 inverted microscope maintained at 37°C using a Peltier heated coverslip holder. Confocal imaging of the eGFP-tagged biosensors was monitored using either an Olympus FV500 or a PerkinElmer UltraVIEW confocal microscope as previously described (Witherow et al., 2003; Nash et al., 2002). Briefly, eGFP was excited using the 488nm laser line and the emitted fluorescence was captured at wavelengths >505nm, with images collected at 1s intervals. Analysis was carried out using software supplied by the confocal manufacturer (Olympus Fluoview or PerkinElmer Imaging Suite),

with raw fluorescence data exported to Microsoft Excel and expressed as F/F_0 (eGFP fluorescence/basal eGFP fluorescence) for each cell. For Ca^{2+} imaging, cells were loaded with fluo-3 in KHB by incubation with fluo-3-acetoxymethyl ester (fluo-3-AM; TEF labs Austin, TX, U.S.A.; 2 μ M prepared in anhydrous DMSO) for 45min at 20°C followed by a further 45min incubation in KHB to allow de-esterification of the indicator. Measurement of the intracellular Ca^{2+} concentration ($[Ca^{2+}]_i$) was performed using either an Olympus FV500 or PerkinElmer UltraVIEW confocal microscope with images collected every second. On-line analysis and data processing was performed as previously described for eGFP. For imaging experiments, data are reported as the average \pm s.e.m for n cells from at least 3 individual coverslips.

Measurement of total PLC activity - Agonist induced accumulation of [3 H] mono- and polyphosphates of inositol ([3 H]-InsP $_x$) was determined in cells pre-labelled with *myo*-[3 H]-inositol in which inositol monophosphatase activity was blocked with Li $^+$. Cells were pre-labelled with 3 μ Ci/ml of *myo*-[3 H]-inositol (76Ci/mmol) for 48h in 24-well multidishes to ensure equilibrium labelling. On the day of experiments the media was removed and replaced with 250 μ l KHB supplemented with 10mM LiCl. After a 10min incubation, cells were stimulated by the addition of 250 μ l KHB containing Li $^+$ and agonist at twice the required concentration. Stimulations were carried out in triplicate and after a 20min incubation reactions were terminated by the addition of an equal volume of 1M trichloroacetic acid. [3 H]-InsP $_x$ were extracted and separated by anion exchange chromatography exactly as described previously (Wheldon et al., 2001). Experimental data are reported as the mean \pm s.e.m of n experiments.

Data analysis - In all cases data are reported as the mean \pm s.e.m. for n experiments. For imaging experiments n refers to the number of cells for each condition taken from n different coverslips. For experiments measuring total PLC activity, n refers to the number of

different accumulations. Statistical analysis was carried out using one-way ANOVA and where $P < 0.05$ followed by Dunnett's range test. In all cases, * represents $P < 0.05$; ** $P < 0.01$ and *** $P < 0.001$ by the range test.

Results

Transient expression of myc-tagged RGS proteins. In order to determine the expression of RGS proteins and allow expression at equivalent levels where required, a C-terminal *myc*-epitope tag was incorporated into the DNA sequence encoding RGS2, RGS3 and RGS4. Expression of the RGS*myc* fusion proteins allowed subsequent immunoblotting of the *myc*-epitope tag (and hence RGS protein) with an anti-*myc* antibody. In HEK293/M₃ cells transiently transfected with plasmid DNAs, the anti-*myc* antibody recognised proteins at the expected molecular weights for RGS2*myc* (~28kDa), RGS3*myc* (~80kDa) and RGS4*myc* (~28kDa) (Figure 1). Following transfection of either HEK293/M₃ cells (Figure 1) or HEK293/WT cells (data not shown) with identical amounts of plasmid DNAs encoding either RGS2*myc*, RGS3*myc* or RGS4*myc* the expression level of RGS3*myc* (and the LacZ*myc* control) was consistently 2-3 fold greater than either RGS2*myc* or RGS4*myc*.

Sub-cellular localization of RGS proteins. In order to evaluate the sub-cellular distribution of expressed recombinant RGS proteins, HEK293/M₃ cells were transiently transfected with the RGS*myc* DNA constructs and protein localization determined by immunocytochemistry using an anti-*myc* primary antibody and FITC-labelled secondary antibody. The distribution of fluorescence indicated that RGS2*myc* was expressed at high levels in the nucleus compared to the cytoplasm (Figure 2a). In contrast, both RGS3*myc* and RGS4*myc* were predominantly cytosolic (Figure 2b and c). Immunocytochemistry of untransfected cells or addition of the secondary antibody only to transfected cells did not reveal any cellular staining under conditions identical to those used above (data not shown).

Single-cell imaging of Ins(1,4,5)P₃ generation. Protein-based biosensors have recently been developed that can detect the generation of either Ins(1,4,5)P₃ (eGFP-PH_{PLC δ 1}) or diacylglycerol (eGFP-PKC γ C1₂) in real-time at the single-cell level. Here we firstly used eGFP-PH_{PLC δ 1} to determine the ability of either untagged or *myc*-tagged RGS2, RGS3 and

RGS4 to inhibit muscarinic receptor-mediated generation of $\text{Ins}(1,4,5)\text{P}_3$ in HEK293/ M_3 cells. In cells transiently transfected with the eGFP- $\text{PH}_{\text{PLC}\delta 1}$ biosensor alone, challenge with 100 μM methacholine resulted in a rapid and robust translocation of eGFP fluorescence from the membrane to the cytoplasm in all cells examined (e.g. Figure 3a(i)). Determination of the cytosolic fluorescence indicated a rapid, marked and sustained increase in the level of cytosolic fluorescence (Figure 3b) reflective of agonist-mediated $\text{Ins}(1,4,5)\text{P}_3$ accumulation (Nash et al., 2001; Nash et al., 2002). In contrast, in cells co-transfected with both the eGFP- $\text{PH}_{\text{PLC}\delta 1}$ biosensor and RGS3 myc , 100 μM methacholine had no effect on the plasma membrane localization of eGFP fluorescence (Figure 3a(ii) and b) demonstrating a marked inhibition of muscarinic receptor-mediated $\text{Ins}(1,4,5)\text{P}_3$ accumulation. Quantification of the maximal increase in cytosolic fluorescence in the 60s following agonist addition provides an index of the maximal extent of $\text{Ins}(1,4,5)\text{P}_3$ accumulation. Data collected over a series of experiments demonstrated that expression of untagged or myc -tagged versions of either RGS2 or RGS3 markedly inhibited $\text{Ins}(1,4,5)\text{P}_3$ responses to maximal activation of muscarinic receptors in HEK293/ M_3 cells (Figure 3c). In contrast, expression of either RGS4 or RGS4 myc did not affect the magnitude of $\text{Ins}(1,4,5)\text{P}_3$ responses to 100 μM methacholine (Figure 3c).

The expression level of RGS3 myc determines the extent of inhibition of agonist-mediated $\text{Ins}(1,4,5)\text{P}_3$ generation. In the experiments described above, the transient transfection of HEK293/ M_3 cells with matched levels of DNA for the different RGS myc constructs resulted in a higher level of expression of RGS3 myc compared with either RGS2 myc or RGS4 myc (Figure 1). In additional experiments we therefore reduced the amount of RGS3 myc plasmid DNA used in the transfection in an effort to lower the expression level of RGS3 myc to levels equivalent with RGS2 myc and RGS4 myc . Western blotting of cell lysates following transfection demonstrated that reducing the amount of

RGS3myc plasmid DNA resulted in a reduced level of RGS3myc expression (Figure 4a). Densitometric analysis of Western blots indicated that HEK293/M₃ cells transfected with 0.5µg/well of RGS3myc plasmid DNA expressed approximately equivalent levels of RGSmyc protein as cells transfected with 1.5µg/well of either RGS2myc or RGS4myc DNA (data not shown). Functional experiments with eGFP-PH_{PLCδ1} demonstrated that with increasing amounts of transfected RGS3myc plasmid DNA, the degree of inhibition of Ins(1,4,5)P₃ increased (Figure 4b). At a concentration of 0.5µg/well of RGS3myc plasmid DNA, there was partial (~50%) inhibition of Ins(1,4,5)P₃ accumulation in response to a maximal concentration of methacholine (100µM) but a complete inhibition of signaling in response to a sub-maximal (~EC₅₀) concentration of methacholine (1µM) (Figure 4b). One consideration is that at lower amounts of RGS3myc plasmid DNA there were fewer cells expressing both the eGFP-PH_{PLCδ1} biosensor and RGS3myc. However, in similar studies in which we varied the amount of RGS3myc plasmid DNA, the proportion of cells expressing RGS3myc, as assessed by immunocytochemistry, were similar (data not shown). Furthermore, in the functional studies using the eGFP-PH_{PLCδ1} biosensor there was no evidence for the emergence of two distinct populations of cells (i.e. those in which signaling was inhibited and those in which it was not) (Figure 4c). Concentration-response curves for methacholine-mediated membrane to cytosol translocation of the eGFP-PH_{PLCδ1} biosensor demonstrated that the expression of either LacZmyc or RGS4myc (1.5µg plasmid DNA/well) did not affect agonist-mediated Ins(1,4,5)P₃ accumulation (Figure 5). This was reflected in E_{max} values and pEC₅₀ values that were not significantly different from those in cells transfected with the biosensor alone (pEC₅₀ values: control, 6.4±0.1 (n=3); LacZmyc, 6.1±0.1 (n=3); RGS4myc, 6.3±0.3 (n=3)). The expression of RGS2myc and RGS3myc (1.5µg plasmid DNA/well) did, however, reduce the E_{max} of methacholine-mediated Ins(1,4,5)P₃ accumulation (Figure 5). The extent of the inhibitory effect of RGS3myc was dependent

upon the level of expression. Thus, when the expression levels of RGS2myc and RGS3myc were matched (by reducing the RGS3myc plasmid DNA to 0.5µg plasmid DNA/well) the extent of inhibition by RGS2myc and RGS3myc were approximately equivalent (Figure 5). Although both RGS2myc and RGS3myc reduced the E_{\max} of responses, agonist potency was unaffected compared to controls (pEC₅₀ values: RGS2myc, 6.4±0.1 (n=3); RGS3myc 0.5µg plasmid DNA/well, 6.3±0.3 (n=3); RGS3myc 1.5µg plasmid DNA/well, 5.8±0.1 (n=3)). In addition to inhibiting the magnitude of muscarinic receptor-mediated Ins(1,4,5)P₃ responses, RGS2myc and RGS3myc inhibited the rate of Ins(1,4,5)P₃ generation at both sub-maximal (1µM) and maximal (100µM) concentrations of methacholine as implied by reductions in the rate of change of the cytosolic fluorescence (Table 1). Although RGS4myc did not influence the maximal change in cytosolic fluorescence at any concentration of methacholine, it did reduce the rate of change at both sub-maximal and maximal concentrations of methacholine (Table 1).

Single-cell imaging of diacylglycerol production. To assess the potential impact of the RGS proteins on the other limb of the signaling pathway resulting from PLC-mediated hydrolysis of PtdIns(4,5)P₂, and to confirm that the effects were not specific to the eGFP-PH_{PLCδ1} biosensor, we next assessed the effects of RGSmyc proteins on muscarinic receptor-mediated diacylglycerol production using the eGFP-PKCγC1₂ biosensor. Transient transfection of eGFP-PKCγC1₂ in HEK293/M₃ cells resulted in the expression of cytosolic fluorescence that translocated to the plasma membrane upon addition of 100µM methacholine in all cells (Figure 6a(i)). Determination of the cytosolic fluorescence showed that the agonist-mediated loss of cytosolic fluorescence occurred immediately on agonist addition, was maximal by approximately 20s but largely restored over the subsequent 140s despite the continued presence of methacholine (Figure 6b). The co-expression of RGS3myc with the eGFP-PKCγC1₂ biosensor abolished the cytosol to membrane translocation of eGFP

fluorescence upon addition of 100 μ M methacholine (Figure 6a(ii) and b) indicating marked inhibition of diacylglycerol accumulation. The expression of RGS2 myc also significantly inhibited translocation of eGFP fluorescence in response to 100 μ M methacholine (Figure 6c). In contrast, expression of RGS4 myc did not influence the response (Figure 6c).

Generation of HEK293 cell lines with stable expression of RGS myc proteins. In order to overcome the limitations of transient transfection protocols (e.g. potentially variable transfection efficiency and a limited ability to carry out population-based measurements) we generated HEK293 cell lines with stable expression of RGS2 myc , RGS3 myc or RGS4 myc . Transfection of HEK293/WT cells with RGS myc plasmid DNAs resulted in the generation of cell lines from which single clones of cells expressing either RGS2 myc (HEK293/RGS2 myc), RGS3 myc (HEK293/RGS3 myc) or RGS4 myc (HEK293/RGS4 myc) were selected on the basis of similar expression levels of the myc -tagged proteins (Figure 7a). HEK cells endogenously express the muscarinic M₃ receptor (Ancellin et al., 1999). Following selection, the expression of endogenous muscarinic receptors was assessed using [³H]-NMS binding to intact cells. Each of the cell lines had expression levels similar to HEK293/WT (~40 fmol/mg total cell protein; data not shown). Furthermore, levels of G $\alpha_{q/11}$ were similar as assessed by immunoblotting with a previously characterised antibody (Mitchell et al., 1991) (data not shown). Immunocytochemistry demonstrated that the sub-cellular distribution of the stably expressed RGS myc proteins was identical to their distribution when expressed transiently (see Figure 2).

Receptor-mediated PLC activity in cell lines having stable expression of RGS myc proteins. Transfection of the eGFP-PH_{PLC δ 1} biosensor plasmid DNA into HEK/WT cells results in the expression of membrane-localized fluorescence identical to that seen in HEK293/M₃ cells. However, activation of the endogenously expressed muscarinic receptors with 100 μ M methacholine caused little or no membrane to cytosol translocation in these

cells. This is consistent with a lack of methacholine-mediated accumulation of Ins(1,4,5)P₃ mass in populations of these cells (data not shown) measured using a well characterised radioreceptor assay (Willars and Nahorski, 1995). In contrast, 100μM methacholine evoked an accumulation of [³H]-InsP_x against a Li⁺-block of inositol monophosphatase in these cells. Accumulation of [³H]-InsP_x in such experiments is independent of the metabolism of Ins(1,4,5)P₃ and reflects total PLC activity (Willars et al., 1998). A 20min stimulation of HEK293/WT cells with either 1μM or 100μM methacholine resulted in a 2.5±0.1 (n=5) and 8.1±0.5 (n=5) fold-over basal accumulation of [³H]-InsP_x respectively (Figure 7b). The extent of accumulation was similar in cells expressing RGS4myc but significantly reduced in cells expressing RGS2myc and essentially abolished in cells expressing RGS3myc (Figure 7b). The direct stimulation of G-proteins with aluminium fluoride (AlF₄⁻) also caused a 3.1±0.1 (n=3) fold-over basal accumulation of [³H]-InsP_x over a 30min period (Figure 7b). This AlF₄⁻-mediated accumulation of [³H]-InsP_x was, however, unaffected by the expression of RGS2myc, RGS3myc or RGS4myc in the clonal cell lines (Figure 7b).

The effect of RGS proteins on the amplitude, kinetics and pattern of receptor-mediated Ca²⁺ signals. Single cell imaging of intracellular Ca²⁺ signaling in HEK293/WT cells revealed that low concentrations of methacholine (1μM) caused repetitive whole-cell Ca²⁺ oscillations that subsided gradually with time and in which the [Ca²⁺]_i returned to approximately basal levels between oscillations (Figure 8 a(i)). In cells expressing either RGS2myc, RGS3myc or RGS4myc there were significant reductions in both the magnitude of the initial Ca²⁺ response (Figure 8a(i-iv) and Figure 9a) and the rise-time of the initial peak (Figure 9b) in response to this sub-maximal concentration of methacholine (1μM). Expression of the RGS proteins was also associated with a dampening of the magnitude and frequency of subsequent oscillations (Figure 8a(i-iv) and Figure 9c). A higher concentration of methacholine (100μM) resulted in more robust Ca²⁺ signaling in HEK293/WT cells

(compare Figures 8a(i) and 8b(i)). The majority of cells responded with a rapid peak of Ca^{2+} elevation followed by a more sustained phase, although some cells oscillated around this elevated level. In cells expressing either RGS2*myc* or RGS3*myc* there were significant reductions in the amplitude and rise-time of the initial peak response (Figure 9a and b). However, expression of these RGS proteins resulted in an increase in oscillatory behaviour (Figure 8b(i-iii) and Figure 9c). RGS4*myc* did not affect either the amplitude or rise-time of the initial peak Ca^{2+} response to 100 μM methacholine (Figure 8b(i and iv), Figure 9a and b), although a slight increase in oscillatory behaviour was observed (Figure 8b(i and iv)).

RGS proteins inhibit Ca^{2+} signals mediated by the endogenous $\text{G}\alpha_{q/11}$ -coupled P2Y_2 receptor. There is some evidence that RGS proteins are selective amongst different receptor types that couple to $\text{G}\alpha_{q/11}$ (Zeng et al., 1998; Xu et al., 1999) and recent evidence has suggested that this may be a consequence of interactions between the GPCR and RGS protein (Bernstein et al., 2004). HEK293 cells also express endogenous P2Y_2 nucleotide receptors that couple to $\text{G}\alpha_{q/11}$ (Werry et al., 2002) and we therefore carried out a preliminary investigation of the impact of RGS protein expression on signaling by these receptors. Stimulation of P2Y_2 nucleotide receptors with a maximal concentration of UTP resulted in $[\text{Ca}^{2+}]_i$ responses similar to those seen with 100 μM methacholine (data not shown). UTP-mediated Ca^{2+} signaling was also inhibited by expression of RGS2*myc* and even more so by RGS3*myc* as judged by reductions in the amplitude of the initial peak response (Figure 9d). However, RGS4*myc* had no effect on the Ca^{2+} responses to this maximal concentration of UTP (Figure 9d).

Following addition of AlF_4^- to HEK293/WT cells there was a lag period of $105 \pm 8\text{s}$ ($n=15$) before the appearance of baseline Ca^{2+} oscillations (Figure 10a) that were similar to those evoked by a low concentration (1 μM) of methacholine (Figure 8a(i)). The amplitude of the initial Ca^{2+} response to AlF_4^- was not significantly affected by the expression of the

RGS myc proteins (Figure 10b and c). Furthermore oscillation frequency was not affected (HEK293/WT, 1.69 ± 0.09 oscillations in 100s (n=48); RGS2 myc , 1.67 ± 0.14 (n=30); RGS3 myc , 1.74 ± 0.07 (n=38); RGS4 myc , 1.54 ± 0.08 s (n=48)). However, the lag phase between the addition of AlF_4^- and the first Ca^{2+} response was significantly longer in the RGS myc -expressing cell lines (RGS2 myc , 173 ± 5 (n=27); RGS3 myc , 218 ± 8 s (n=15); RGS4 myc , 177 ± 6 s (n=44); all $P < 0.001$ vs. HEK293/WT cells).

The effect of RGS proteins on PLC signaling mediated by constitutively active $G\alpha_q$.

Next we sought to establish the impact of RGS myc protein expression on signaling mediated by a CA- $G\alpha_q$ (Q209L) that is insensitive to the GTPase activity of RGS proteins (Heximer et al., 2001). In HEK293/WT cells transiently transfected with CA- $G\alpha_q$ (0.25 μ g/well of a 24-well multi-dish), the addition of 10mM Li^+ to block inositol monophosphatase activity for 20min resulted in a 3.6 ± 0.4 (n=3) fold increase in $^3[H]$ -InsP $_x$ accumulation compared to control, untransfected cells. Addition of Li^+ to cells with transient expression of CA- $G\alpha_q$ and stable expression of one of the RGS myc proteins also resulted in the accumulation of $^3[H]$ -InsP $_x$ (Figure 11). The accumulation of $^3[H]$ -InsP $_x$ was significantly greater in cell lines expressing either RGS2 myc or RGS3 myc compared to either HEK293/WT cells or cells expressing RGS4 myc (Figure 11).

Discussion

Here we have compared the abilities of members of the B/R4 family of RGS proteins to inhibit Ca^{2+} and phosphoinositide signaling by $\text{G}\alpha_{q/11}$ -coupled muscarinic receptors. We selected RGS4 as the prototypical member of the B/R4 family along with RGS2 given its high specificity for $\text{G}\alpha_q$ (Heximer et al., 1997). We also selected RGS3, as although its RGS domain has high homology with other family members, it is atypical in having a large N-terminal of unknown function (Hollinger and Hepler, 2002). Previous studies suggest that each of these RGS proteins influence $\text{G}\alpha_{q/11}$ signaling (Hollinger and Hepler, 2002) and that RGS2 and RGS4 have different inhibitory activities (Heximer et al., 1997).

Within the present study we have made use of single cell imaging techniques to enable a more precise understanding of the influence of the RGS proteins on the magnitude and kinetics of signaling. In particular this has allowed the determination of the effects of RGS proteins on PLC-mediated signaling in the seconds immediately following receptor activation. This is of considerable importance given that the vast majority of PLC-coupled GPCRs undergo either a full or partial desensitisation within seconds of agonist addition, most likely through receptor phosphorylation. The muscarinic M_3 receptor is a well-studied example of such a receptor, having an initial, rapidly desensitised component of signaling followed by a sustained, desensitisation-resistant phase. Many previous studies examining the effects of RGS proteins on PLC have determined inositol phosphate accumulation against a Li^+ -block of inositol monophosphatase over many minutes. This will not reflect the levels of the second messenger, $\text{Ins}(1,4,5)\text{P}_3$, nor will it reflect the impact of RGS proteins on the immediate, likely physiologically relevant phase of receptor activation. Furthermore, the initial and sustained phases of receptor signaling can be driven with different agonist potencies (Willars and Nahorski, 1995) and are clearly subject to different regulatory features.

RGS2 and RGS3 inhibited both the magnitude and rate of the immediate, agonist-induced $\text{Ins}(1,4,5)\text{P}_3$ generation in single cells during maximal receptor activation as assessed using the eGFP- $\text{PH}_{\text{PLC}\delta 1}$ biosensor. In contrast, RGS4 had no effect on the magnitude but more subtly reduced the rate of generation. Importantly, the effects of the *myc*-tagged and untagged RGS proteins were identical. This is consistent with other studies in which RGS2 and RGS4 have been similarly tagged without consequence (Heximer et al., 1999; Srinivasa et al., 1998).

Although muscarinic receptor-mediated $\text{Ins}(1,4,5)\text{P}_3$ accumulation was inhibited in the order $\text{RGS3} > \text{RGS2} > \text{RGS4}$, immunoblotting showed RGS3myc expression was greater than either RGS2myc or RGS4myc . Interestingly, untagged versions showed similar levels of inhibition to their *myc*-tagged counterparts suggesting similar differences in expression levels and that these are a feature of the RGS proteins. This could reflect interactions with other proteins, which can result in stabilization of the RGS protein (Witherow et al., 2000). Reducing the amount of transfected DNA reduced both the expression of RGS3myc and the inhibition of receptor-mediated $\text{Ins}(1,4,5)\text{P}_3$ generation. At approximately equivalent expression levels, inhibition by RGS3myc was more consistent with that of RGS2myc . Despite effects of RGS2myc and RGS3myc on $\text{Ins}(1,4,5)\text{P}_3$ generation, agonist potency was unaffected.

We also used the eGFP- $\text{PKC}\gamma\text{C1}_2$ biosensor to examine diacylglycerol formation, which is complimentary to $\text{Ins}(1,4,5)\text{P}_3$ but has distinct signaling consequences. When expressed at similar levels, RGS2myc and RGS3myc but not RGS4myc inhibited diacylglycerol formation as assessed by reduced cytosol to membrane translocation of eGFP- $\text{PKC}\gamma\text{C1}_2$.

To increase the utility of our model, we generated stable cell lines from HEK293/WT cells that expressed the RGSmyc proteins at similar levels. RGS2myc and RGS3myc reduced

both the amplitude and kinetics of single cell Ca^{2+} events at maximal and sub-maximal agonist concentrations. In contrast, inhibitory effects of RGS4 $_{myc}$ were only apparent at sub-maximal agonist concentrations. The RGS proteins also influenced the patterns of Ca^{2+} signaling. At low agonist concentrations that produced oscillatory Ca^{2+} patterns in HEK293/WT cells, the RGS $_{myc}$ proteins dampened both the amplitude and frequency of oscillations. In contrast, at high agonist concentrations, that produced essentially peak and sustained Ca^{2+} responses in HEK293/WT cells, RGS $_{myc}$ expression promoted oscillatory Ca^{2+} signaling. The pattern of Ca^{2+} signaling is key in defining the cellular responses to agonist stimulation and the demonstration that RGS proteins can influence the pattern as well as the extent of Ca^{2+} signaling has important physiological implications. The precise mechanisms underlying oscillatory Ca^{2+} signaling are unclear. Low levels of $\text{Ins}(1,4,5)\text{P}_3$ may sensitize its receptor to Ca^{2+} -induced Ca^{2+} release and promote regenerative Ca^{2+} oscillations, whereas at higher levels a dynamic (oscillatory) uncoupling of the GPCR signaling complex (e.g. receptor phosphorylation/ dephosphorylation) may regulate oscillations (Nash et al., 2002). At still higher levels of $\text{Ins}(1,4,5)\text{P}_3$, its receptors may saturate, causing peak and plateau Ca^{2+} responses. In our studies, reduced $\text{Ins}(1,4,5)\text{P}_3$ could account for RGS protein effects at both low and high agonist concentrations. We cannot, however, exclude the possibility that oscillatory changes in $\text{G}\alpha_{q/11}$ activation caused by cycles of activation and inactivation of RGS proteins cause oscillatory Ca^{2+} signaling as recently suggested (Luo et al., 2001).

The greater inhibitory activity of RGS2 compared to RGS4 is consistent with an earlier cellular study that examined inositol phosphate accumulation (Heximer et al., 1999) but in contrast to that observed *in vitro* (RGS2>RGS3=RGS4) (Heximer et al., 1997; Scheschonka et al., 2000). This suggests that other factors may determine RGS protein specificity *in vivo* and this could involve interactions with other molecules. An obvious

candidate is the GPCR, as recently demonstrated for RGS2 and the third intracellular loop of the $G\alpha_{q/11}$ -coupled muscarinic M_1 receptor (Bernstein et al., 2004). Interestingly, RGS2 but not RGS4 also interacts with this region of the muscarinic M_3 receptor (Bernstein et al., 2004). We were, however, unable to obtain any evidence for differences in the sub-cellular localisation of the RGS proteins that could easily account for their different inhibitory properties. Thus, immunocytochemistry revealed that, as in previous studies (De Vries et al., 2000; Roy et al., 2003), RGS2*myc* is highly expressed in the nucleus, whilst both RGS3*myc* and RGS4*myc* are predominantly cytosolic.

To determine if effector antagonism could account for RGS protein action we examined their impact on GAP-resistant G-protein activation using either AlF_4^- to directly activate G-proteins or a constitutively active $G\alpha_q$ (CA- $G\alpha_q$; Q209L) that is resistant to RGS protein GAP activity (Heximer et al., 2001). RGS protein expression did not affect AlF_4^- -mediated [3H]-InsP $_x$ accumulation. Furthermore, although RGS proteins increased the delay prior to AlF_4^- -evoked Ca^{2+} oscillations, they did not affect either their frequency or amplitude. This suggests that GAP activity may be required to influence agonist-mediated oscillatory Ca^{2+} signals. The reason for the increased delay is unclear but could reflect binding of RGS proteins to inactive G-protein α -subunits (Roy et al., 2003). Thus, the release of α -subunits could be delayed during AlF_4^- stimulation but not agonist stimulation when the receptor acts as a guanine-nucleotide exchange factor (i.e. GDP-GTP exchange is not limiting). An additional factor that may complicate interpretation is that RGS proteins bind with higher affinity to G-proteins in the GDP- AlF_4^- -bound state than the GTP-bound state (Ross and Wilkie, 2000). A final point limiting the usefulness of AlF_4^- is that it activates all heterotrimeric G-proteins and those other than $G\alpha_{q/11}$ may contribute to the measured responses through, for example the activation of PLC by $G\beta\gamma$ -subunits. Thus, as an alternative approach we used CA- $G\alpha_q$ that in addition to being GAP-resistant has an affinity

for RGS proteins consistent with GTP-bound $G\alpha$ -subunits (Ross and Wilkie, 2000), making it useful in the examination of effector antagonism. Transient transfection of CA- $G\alpha_q$ into HEK293/WT cells markedly increased PLC activity as judged from the accumulation of [3 H]-InsP $_x$ against a Li $^+$ -block. Expression of CA- $G\alpha_q$ in the RGS myc expressing cell lines similarly enhanced [3 H]-InsP $_x$ accumulation. Direct comparison of stimulation levels may be complicated by reciprocal effects of RGS proteins and $G\alpha$ -subunits on expression levels (Anger et al., 2004). However, these data demonstrate that effector antagonism is insufficient to fully block G-protein-mediated activation of PLC. Of note, CA- $G\alpha_q$ caused robust accumulation of [3 H]-InsP $_x$ in RGS3 myc -expressing cells despite almost no muscarinic receptor-mediated accumulation. Thus, RGS proteins were unable to efficiently block signaling by CA- $G\alpha_q$. Extrapolation to the effects of RGS proteins on endogenous G-proteins expressed at lower levels is difficult and we cannot exclude the possibility that effector antagonism accounts for a proportion of the effects on receptor-mediated signaling. Indeed a recent study suggested that GAP-independent mechanisms of RGS2 and RGS3 inhibited signaling by muscarinic M $_3$ receptors when over-expressed in COS-7 cells (Anger et al., 2004). However, the contribution of effector antagonism versus GAP activity for endogenously expressed RGS proteins acting on endogenously expressed receptors remains to be defined.

In conclusion, along with population-based biochemical assays we used a Ca $^{2+}$ -sensitive dye and novel biosensors to detect [Ca $^{2+}$] $_i$, Ins(1,4,5)P $_3$ and diacylglycerol production to assess RGS-mediated inhibition of $G\alpha_{q/11}$ -mediated signaling at the single-cell level in live cells and in real time. This allowed a detailed examination of the effects of RGS proteins not only on the magnitude of GPCR-mediated signaling but also on the kinetics and temporal profiles.

References

- Ancellin, N., Preisser, L., Le Maout, S., Barbado, M., Créminon, C., Corman, B. and Morel, A. (1999) Homologous and heterologous phosphorylation of the vasopressin V1a receptor. *Cell Signal* **11**: 743-751.
- Anger T, Zhang W, and Mende U (2004) Differential contribution of GTPase activation and effector antagonism to the inhibitory effect of RGS proteins on G_q-mediated signaling in vivo. *J Biol Chem* **279**, 3906-3915.
- Bernstein LS, Ramineni S, Hague C, Cladman W, Chidiac P, Levey AI and Hepler JR (2004) RGS2 binds directly and selectively to the M1 muscarinic acetylcholine receptor third intracellular loop to modulate G_{q/11α} signaling. *J Biol Chem* **279**: 21248–21256.
- Castro-Fernandez C, and Conn PM (2002) Regulation of the gonadotropin-releasing hormone receptor (GnRHR) by RGS proteins: role of the GnRHR carboxyl-terminus. *Mol Cell Endocrinol* **191**: 149-156.
- De Vries L, Zheng B, Fischer T, Elenko E, and Farquhar MG (2000) The regulator of G protein signaling family. *Ann Rev Pharmacol Toxicol* **40**: 235-271.
- Doupnik CA, Davidson N, Lester HA, and Kofuji P (1997) RGS proteins reconstitute the rapid gating kinetics of Gβγ-activated inwardly rectifying K⁺ channels. *Proc Natl Acad Sci (USA)* **94**: 10461-10466.
- Hepler JR (1999) Emerging roles for RGS proteins in cell signalling. *Trends Pharmacol Sci* **20**: 376-382.
- Heximer SP, Watson N, Linder ME, Blumer KJ. and Hepler JR (1997) RGS2/G0S8 is a selective inhibitor of Gqα function. *Proc Natl Acad Sci (USA)* **94**: 14389-14393.

Heximer SP, Srinivasa SP, Bernstein LS, Bernard JL, Linder ME, Hepler JR, and Blumer KJ (1999) G protein selectivity is a determinant of RGS2 function. *J Biol Chem* **274**: 34253-34259.

Heximer SP, Lim H, Bernard JL, and Blumer KJ (2001) Mechanisms governing subcellular localization and function of human RGS2. *J Biol Chem* **276**: 14195-14203.

Hollinger S, and Hepler JR (2002) Cellular regulation of RGS proteins: Modulators and integrators of G protein signaling. *Pharmacol Rev* **54**: 527-559.

Luo X, Popov S, Bera AK, Wilkie TM, and Muallem S (2001) RGS proteins provide biochemical control of agonist-evoked $[Ca^{2+}]_i$ oscillations. *Mol Cell* **7**: 651-660.

Mitchell FM, Mullaney I, Godfrey PP, Arkinstall SJ, Wakelam MJO, and Milligan G (1991) Widespread distribution of Gq α /G11 α detected immunologically by an antipeptide antiserum directed against the predicted C-terminal decapeptide. *FEBS Lett* **287**: 171-174.

Nahorski SR, Young KW, Challiss RAJ, and Nash MS (2003) Visualizing phosphoinositide signalling in single neurons gets a green light. *Trends Neurosci* **26**: 444-452.

Nash MS, Young KW, Willars GB, Challiss RA, and Nahorski SR (2001) Single-cell imaging of graded Ins(1,4,5)P₃ production following G-protein-coupled-receptor activation. *Biochem J* **356**: 137-142.

Nash MS, Schell MJ, Atkinson PJ, Johnston NR, Nahorski SR, and Challiss RAJ (2002) Determinants of metabotropic glutamate receptor-5-mediated Ca²⁺ and inositol 1,4,5-trisphosphate oscillation frequency - Receptor density versus agonist concentration. *J Biol Chem* **277**: 35947-35960.

Neill JD, Duck LW, Sellers JC, Musgrove LC, Scheschonka A, Druey KM, and Kehrl JH (1997) Potential role for a regulator of G protein signaling (RGS3) in

gonadotropin-releasing hormone (GnRH) stimulated desensitization. *Endocrinol* **138**: 843-846.

Oancea E, and Meyer T (1998) Protein kinase C as a molecular machine for decoding calcium and diacylglycerol signals. *Cell* **95**: 307-318.

Oancea E, Teruel MN, Quest AF, and Meyer T J (1998) Green fluorescent protein (GFP)-tagged cysteine-rich domains from protein kinase C as fluorescent indicators for diacylglycerol signaling in living cells. *J Cell Biol* **140**: 485-498.

Ross EM, and Wilkie TM (2000) GTPase-activating proteins for heterotrimeric G proteins: Regulators of G protein signaling (RGS) and RGS-like proteins. *Ann Rev Biochem* **69**: 795-827.

Roy AA, Lemberg KE, and Chidiac P (2003) Recruitment of RGS2 and RGS4 to the plasma membrane by G proteins and receptors reflects functional interactions. *Mol Pharmacol* **64**: 587-593.

Rumenapp U, Asmus M, Schablowski H, Woznicki M, Han L, Jakobs KH, Fahimi-Vahid M, Michalek C, Wieland T. and Schmidt M (2001) The M₃ muscarinic acetylcholine receptor expressed in HEK-293 cells signals to phospholipase D via G₁₂ but not G_q-type G proteins - Regulators of G proteins as tools to dissect pertussis toxin-resistant G proteins in receptor-effector coupling. *J Biol Chem* **276**: 2474-2479.

Scheschonka A, Dessauer CW, Sinnarajah S, Chidiac P, Shi CS, and Kehrl JH (2000) RGS3 is a GTPase-activating protein for G_i α and G_q α and a potent inhibitor of signaling by GTPase-deficient forms of G_q α and G₁₁ α . *Mol Pharmacol* **58**: 719-728.

Snow BE, Krumins AM, Brothers GM, Lee SF, Wall MA, Chung S, Mangion J, Arya S, Gilman AG, and Siderovski DP (1998a) A G protein γ subunit-like domain shared between RGS11 and other RGS proteins specifies binding to G β_5 subunits. *Proc Natl Acad Sci (USA)* **95**: 13307-13312.

Snow BE, Hall RA, Krumins AM, Brothers GM, Bouchard D, Brothers CA, Chung S, Mangion J, Gilman AG, Lefkowitz RJ, and Siderovski DP (1998b) GTPase activating specificity of RGS12 and binding specificity of an alternatively spliced PDZ (PSD-95/Dlg/ZO-1) domain. *J Biol Chem* **273**: 17749-17755.

Srinivasa SP, Watson N, Overton MC, and Blumer KJ (1998) Mechanism of RGS4, a GTPase-activating protein for G protein α subunits. *J Biol Chem* **273**: 1529-1533.

Stauffer TP, Ahn S, and Meyer T (1998) Receptor-induced transient reduction in plasma membrane PtdIns(4,5)P₂ concentration monitored in living cells. *Curr Biol* **8**: 343-346.

Tovey SC, de Smet P, Lipp P, Thomas D, Young KW, Missiaen L, De Smedt H, Parys JB, Berridge MJ, Thuring J, Holmes A, and Bootman MD (2001) Calcium puffs are generic InsP₃-activated elementary calcium signals and are downregulated by prolonged hormonal stimulation to inhibit cellular calcium responses. *J Cell Sci* **114**: 3979-3989.

Werry TD, Christie MI, Dainty IA, Wilkinson GF, and Willars GB (2002) Ca²⁺ signalling by recombinant human CXCR2 chemokine receptors is potentiated by P2Y nucleotide receptors in HEK cells. *Br J Pharmacol* **135**: 1199-1208.

Wheldon LM, Nahorski SR, and Willars GB (2001) Inositol 1,4,5-trisphosphate independent calcium signalling by platelet-derived growth factor in the human SH-SY5Y neuroblastoma cell. *Cell Calcium* **30**: 95-106.

Willars GB, and Nahorski SR (1995) Quantitative comparisons of muscarinic and bradykinin receptor-mediated Ins(1,4,5)P₃ accumulation and Ca²⁺ signalling in human neuroblastoma cells. *Br J Pharmacol* **114**: 1133-1142.

Willars GB, Nahorski SR, and Challiss RAJ (1998) Differential regulation of muscarinic acetylcholine receptor-sensitive polyphosphoinositide pools and consequences for signaling in human neuroblastoma cells. *J Biol Chem* **273**: 5037-5046.

Willars GB, McArdle CA, and Nahorski SR (1998) Acute desensitization of phospholipase C-coupled muscarinic M3 receptors but not gonadotropin-releasing hormone receptors co-expressed in α T3-1 cells: implications for mechanisms of rapid desensitization. *Biochem J* **333**: 301-308.

Witherow DS, Wang Q, Levay K, Cabrera JL, Chen J, Willars GB, and Slepak VZ (2000) Complexes of the G protein subunit G β_5 with the regulators of G protein signaling RGS7 and RGS9. Characterization in native tissues and in transfected cells. *J Biol Chem* **275**: 24872-24880.

Witherow DS, Tovey SC, Wang Q, Willars GB, and Slepak VZ (2003) G β_5 -RGS7 inhibits G α_q -mediated signaling via a direct protein-protein interaction. *J Biol Chem* **278**: 21307-21313.

Xu X, Zeng W, Popov S, Berman DM, Davignon I, Yu K, Yowe D, Offermanns S, Muallem S, and Wilkie TM (1999) RGS proteins determine signaling specificity of G $_q$ -coupled receptors. *J Biol Chem* **274**: 3549-3556.

Zeng W, Xu X, Popov S, Mukhopadhyay S, Chidiac P, Swistokl J, Danho W, Yagaloff KA, Fisher SL, Ross EM, Muallem S, and Wilkie TM (1998) The N-terminal domain of RGS4 confers receptor-selective inhibition of G protein signaling. *J Biol Chem* **273**: 34687-34690.

Zheng B, De Vries L, and Gist Farquhar M (1999) Divergence of RGS proteins: evidence for the existence of six mammalian RGS subfamilies. *Trends Biochem Sci* **24**: 411-414.

Footnotes

Financial support of the Biotechnology and Biological Research Council (ref. 91/C15897) and the Wellcome Trust (ref. 061050) is gratefully acknowledged.

Reprint requests to: Dr. Gary. B. Willars, Department of Cell Physiology and Pharmacology, Medical Sciences Building, University of Leicester, University Road, LE1 9HN, United Kingdom. Tel: +44 116 2523094. Fax: +44 116 2525045. E-mail: gbw2@le.ac.uk.

Figure Legends

Figure 1. Transient over-expression of *myc*-tagged RGS proteins.

Western blot of HEK293/M₃ cell lysates (30µg protein/lane), showing the transient over-expression of *myc*-tagged RGS proteins. The number above each lane corresponds to the amount of RGS*myc* DNA transfected. Control lanes are samples from untransfected HEK293/M₃ cells. Blots are representative of cell lysates obtained from at least three different transient transfections.

Figure 2. Sub-cellular localisation of RGS proteins.

Immunolocalisation of RGS2*myc*, RGS3*myc* or RGS4*myc* transiently over-expressed in HEK293/M₃ cells. The *myc*-tag was detected using an anti-*myc* antibody, which was subsequently labelled with a FITC-conjugated secondary antibody. Images are typical of at least three different transient transfections and immuno-labelling experiments.

Figure 3. Single-cell imaging of Ins(1,4,5)P₃ production.

a(i) Typical single-cell confocal images of HEK293/M₃ cells transiently transfected with the Ins(1,4,5)P₃ biosensor, eGFP-PH_{PLCδ1}. Under resting conditions (0s) the eGFP-tagged biosensor is localised to the plasma membrane, but upon agonist stimulation (100µM methacholine) eGFP-PH_{PLCδ1} translocates to the cytosol (20s) corresponding to the production of Ins(1,4,5)P₃. **a(ii)** In HEK293/M₃ cells transiently co-transfected with eGFP-PH_{PLCδ1} and RGS3*myc* the translocation of the eGFP-tagged biosensor is reduced, corresponding to an inhibition of Ins(1,4,5)P₃ production. **b** Sample traces of the change in cytoplasmic eGFP fluorescence with time upon muscarinic M₃ receptor stimulation in HEK293/M₃ cells. Traces represent HEK293/M₃ cells transiently transfected with either

eGFP-PH_{PLC δ 1} alone (upper trace) or cells transiently co-transfected with both eGFP-PH_{PLC δ 1} and RGS3myc (lower trace). The arrow represents the time point for the addition of methacholine (100 μ M). **c** Summary of data from the type of experiments described above. Data represent the mean peak increase in cytoplasmic eGFP fluorescence + s.e.m. for 20-40 cells from at least 4 different coverslips. Statistical comparisons were by one-way ANOVA with Dunnett's range test; * represents $P < 0.05$ and *** $P < 0.001$.

Figure 4. Decreasing RGS3myc expression relieves inhibition of Ins(1,4,5)P₃ generation.

a Immunoblot showing increasing transient expression of RGS3myc in HEK293/M₃ cells with increasing amounts of RGS3myc DNA. The blot is representative of blots from three different transient transfections. **b** Increasing the level of RGS3myc expression in HEK293/M₃ cells leads to a decreased level of Ins(1,4,5)P₃ production. Data represent the mean change in peak cytoplasmic eGFP fluorescence + s.e.m for 20-30 cells from at least 3 different coverslips. **c** Scatter plot of data from Figure 4b. (100 μ M methacholine).

Figure 5. The effect of RGSmyc protein expression on the concentration-dependence of methacholine-mediated Ins(1,4,5)P₃ generation.

Concentration-response curves (0.01-100 μ M methacholine) for single-cell Ins(1,4,5)P₃ production in control HEK293/M₃ cells and HEK293/M₃ cells transiently transfected with either RGS2myc, RGS3myc, RGS4myc or a LacZmyc control vector. Data represent the mean change in cytoplasmic eGFP fluorescence + s.e.m for 20-30 cells from at least 3 different coverslips.

Figure 6. Single-cell imaging of diacylglycerol production.

a(i) Typical single-cell confocal images of HEK293/M₃ cells transiently transfected with the diacylglycerol biosensor eGFP-PKC γ C1₂. Under resting conditions (0s) the eGFP-tagged biosensor is localised homogeneously across the cell cytoplasm and nucleus, but upon agonist stimulation (100 μ M methacholine) the eGFP translocates to the plasma membrane (20s) corresponding to the production of diacylglycerol. **a(ii)** In HEK293/M₃ cells transiently co-transfected with both eGFP-PKC γ C1₂ and RGS3myc the translocation of the eGFP-tagged biosensor is reduced, corresponding to an inhibition of diacylglycerol production. **b** Sample traces of the change in cytoplasmic eGFP fluorescence with time upon muscarinic M₃ receptor stimulation in HEK293/M₃ cells. Traces represent HEK293/M₃ cells transiently transfected with eGFP-PKC γ C1₂ alone (lower trace) and cells transiently co-transfected with both eGFP-PKC γ C1₂ and RGS3myc (upper trace). The arrow represents the time point for the addition of methacholine (100 μ M). **c** Summary of data from the type of experiments described above. Data represent the mean + s.e.m. for 13-30 cells from at least 3 different coverslips. Statistical comparisons were by one-way ANOVA with Dunnett's range test; *** represents P<0.001.

Figure 7. Generation of stable RGSmyc expression in HEK293 cells.

a Western blot of whole cell lysates (20 μ g protein/lane) from HEK293 cells illustrating stable expression of either RGS2myc, RGS3myc or RGS4myc. The blot is representative of at least three different blots for each cell line. **b** Total inositol phosphate ([³H]-InsP_x) accumulation under a Li⁺ block in HEK293/WT, HEK293/RGS2myc, HEK293/RGS3myc and HEK293/RGS4myc cells. Data are shown for stimulation of the endogenous muscarinic M₃ receptor with either 1 or 100 μ M methacholine, and also for receptor-independent activation of G-proteins with AlF₄⁻ (50mM NaF; 50 μ M AlCl₃). Data are represented as the mean +

s.e.m for at least three separate accumulations. Statistical comparisons were by one-way ANOVA with Dunnett's range test; * represents $P < 0.05$ and *** $P < 0.001$.

Figure 8. RGS proteins alter the amplitude, kinetics and pattern of Ca^{2+} signals generated by $\text{G}\alpha_{q/11}$ -coupled receptors.

a (i-iv) Sample traces of Ca^{2+} responses seen in fluo-3 loaded cells (HEK293/WT (i), HEK293/RGS2myc (ii), HEK293/RGS3myc (iii) and HEK293/RGS4myc (iv)) in response to stimulation of the endogenous muscarinic M_3 receptor with a sub-maximal concentration of methacholine (1 μM). **b (i-iv)** Sample traces as described in A (i-iv), but using a maximal concentration of methacholine (100 μM) as the stimulus. The traces illustrate responses from 15-20 cells from one field of view and are typical of traces obtained from at least four different coverslips.

Figure 9. RGS proteins alter the amplitude, kinetics and pattern of Ca^{2+} signals generated by $\text{G}\alpha_{q/11}$ -coupled receptors: summary data.

a The effect of RGSmyc protein expression on the amplitude of the initial Ca^{2+} transient generated in response to stimulation with either 1 or 100 μM methacholine. **b** The effect of RGS protein expression on the kinetics of the initial Ca^{2+} response upon stimulation with 1 or 100 μM methacholine. Data are plotted as 1/rise time (s^{-1}), where the rise time was taken to be the time to reach a peak response from the initial point of inflection. **c** The effect of RGS protein expression on Ca^{2+} oscillations generated in response to prolonged agonist stimulation (1 or 100 μM methacholine). Data represent the number of oscillations seen during a 60s period after the initial Ca^{2+} response. **d** The effect of RGS protein expression on the amplitude of the initial Ca^{2+} signal generated in response to stimulation of endogenous P2Y_2 receptors with 100 μM UTP. In all cases the data represent the mean + s.e.m for between 40 and 100 cells from at least 4 different coverslips.

In Figure 9a and d, data are expressed as the % response relative to control (HEK293/WT cells). Statistical comparisons were by one-way ANOVA with Dunnett's range test; *** represents $P < 0.001$.

Figure 10. RGS proteins do not alter the amplitude or pattern of Ca^{2+} signals generated by direct stimulation of G-proteins with AlF_4^- .

a-b Sample traces of Ca^{2+} transients evoked by AlF_4^- stimulation of HEK293/WT and HEK293/RGS3myc cells respectively. **c** The effect of RGS protein expression on the amplitude of the initial Ca^{2+} signal generated in response to receptor-independent stimulation of G-proteins with AlF_4^- . Data represent the mean + s.e.m for between 40 and 100 cells from at least 4 different coverslips.

Figure 11. The effect of RGS proteins on the activity of a constitutively active form of $\text{G}\alpha_q$ (CA- $\text{G}\alpha_q$).

The accumulation of $[\text{}^3\text{H}]\text{-InsP}_x$ in HEK293/WT, HEK293/RGS2myc, HEK293/RGS3myc and HEK293/RGS4myc transiently transfected with CA- $\text{G}\alpha_q$. Data represent the increase in $[\text{}^3\text{H}]\text{-InsP}_x$ accumulation over a 20min period under Li^+ -block in transfected cells compared to untransfected cells. Data are expressed as the mean + s.e.m for 3 separate accumulations. Statistical comparisons were by one-way ANOVA with Dunnett's range test; ** represents $P < 0.01$ and *** $P < 0.001$.

Table 1

	1μM methacholine	100μM methacholine
Control	0.08 ± 0.01 (n=15)	0.15 ± 0.01 (n=17)
RGS2myc	0.06 ± 0.004 * (n=8)	0.09 ± 0.01 ** (n=15)
RGS3myc (0.5μg)	0.05 ± 0.01 * (n=10)	0.10 ± 0.01 ** (n=12)
RGS3myc (1.5μg)	ND	0.08 ± 0.01 ** (n=4)
RGS4myc	0.04 ± 0.002 *** (n=13)	0.10 ± 0.01 *** (n=19)
LacZmyc	0.08 ± 0.01 (n=14)	0.15 ± 0.01 (n=17)

Table 1. Kinetics of increases in cytosolic fluorescence in response to agonist stimulation in HEK/M₃ cells expressing the Ins(1,4,5)P₃ biosensor, eGFP-PH_{PLCδ1}. Cells transiently transfected with eGFP-PH_{PLCδ1} either alone (control) or with an RGSmyc construct or with a control vector (LacZmyc), were imaged by confocal microscopy and challenged with either 1μM or 100μM methacholine. Data are presented as 1/rise time (s⁻¹), where the rise time was taken to be the time to reach a peak response from the initial point of inflection. Data are mean ± s.e.m, with the number of cells analysed in parentheses. Statistical comparisons were by one-way ANOVA with Dunnett's range test; * represents P<0.05, ** P<0.01 and *** P<0.001.

FIG. 1.

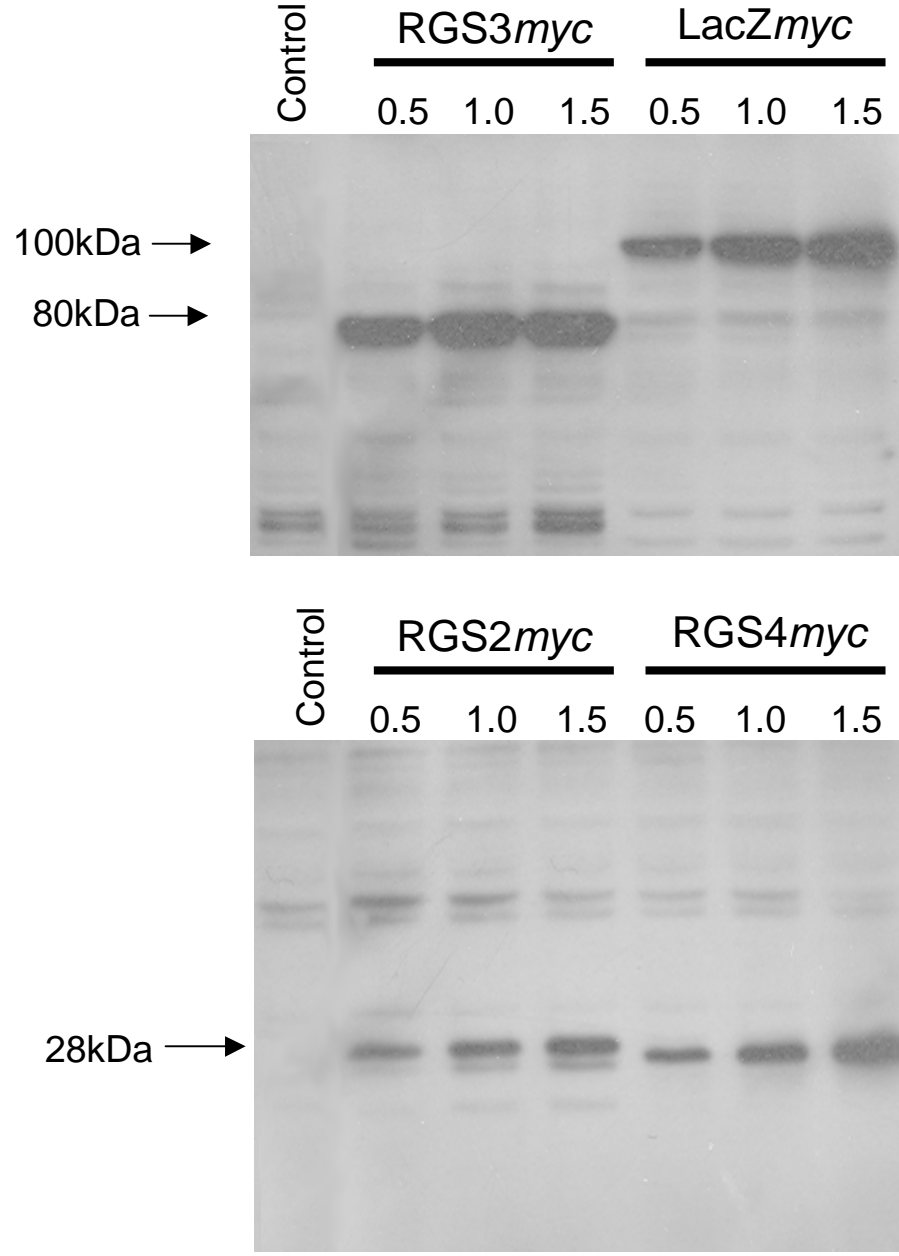


FIG. 2.

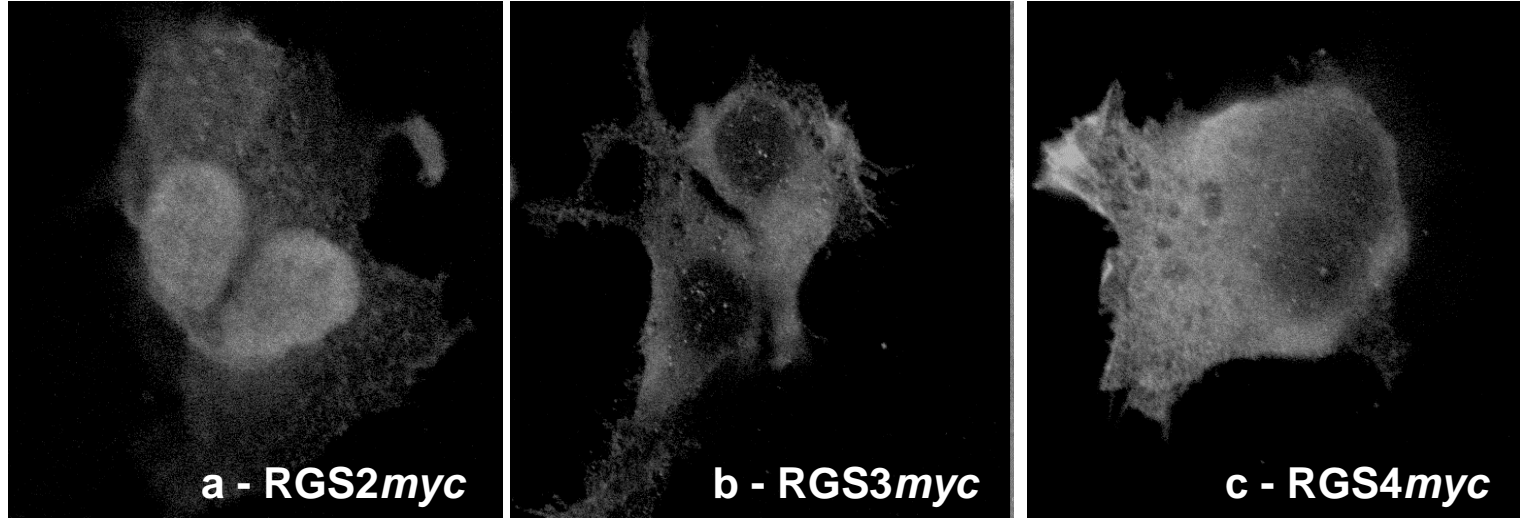


FIG. 3.

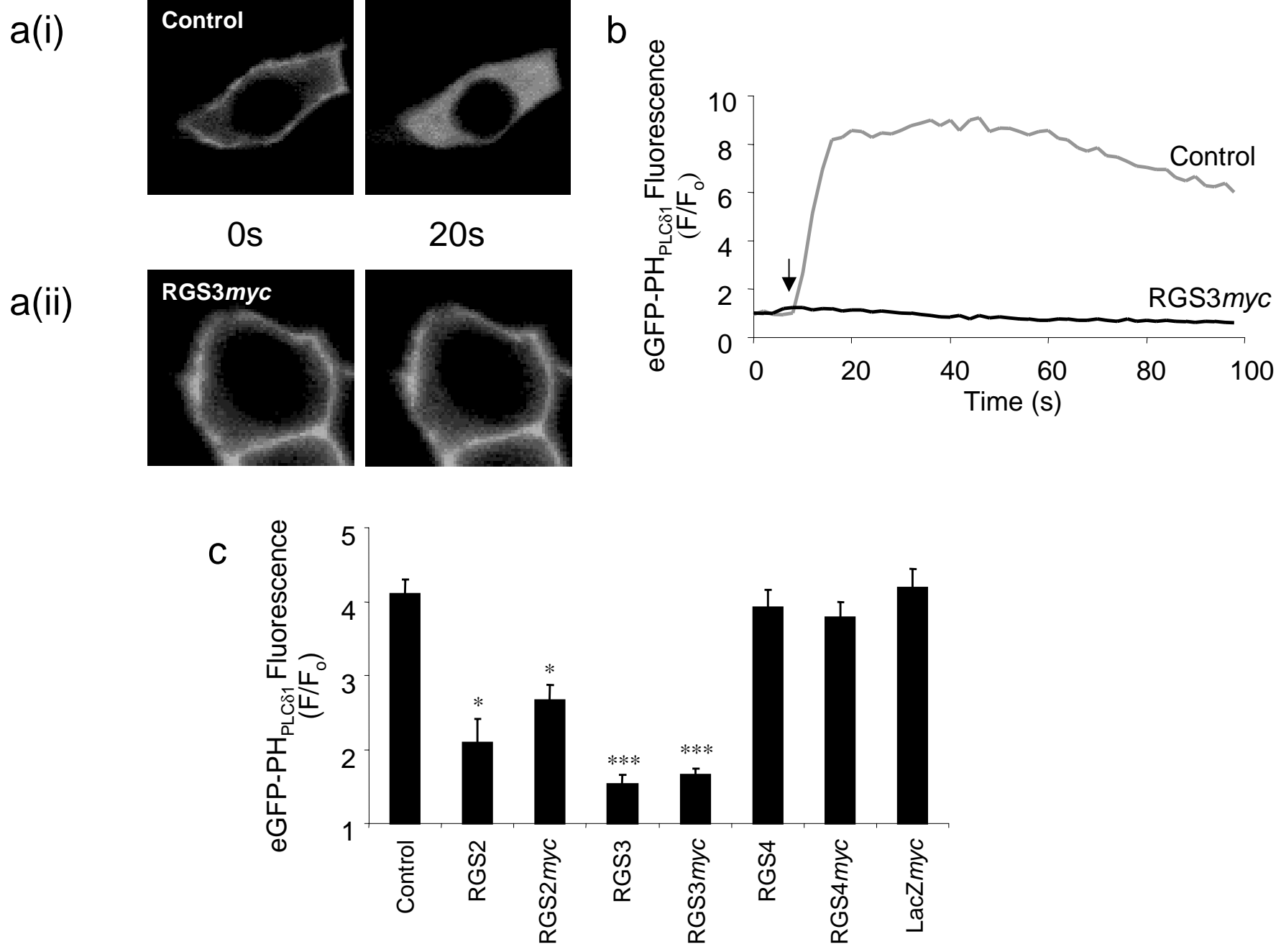


FIG. 4.

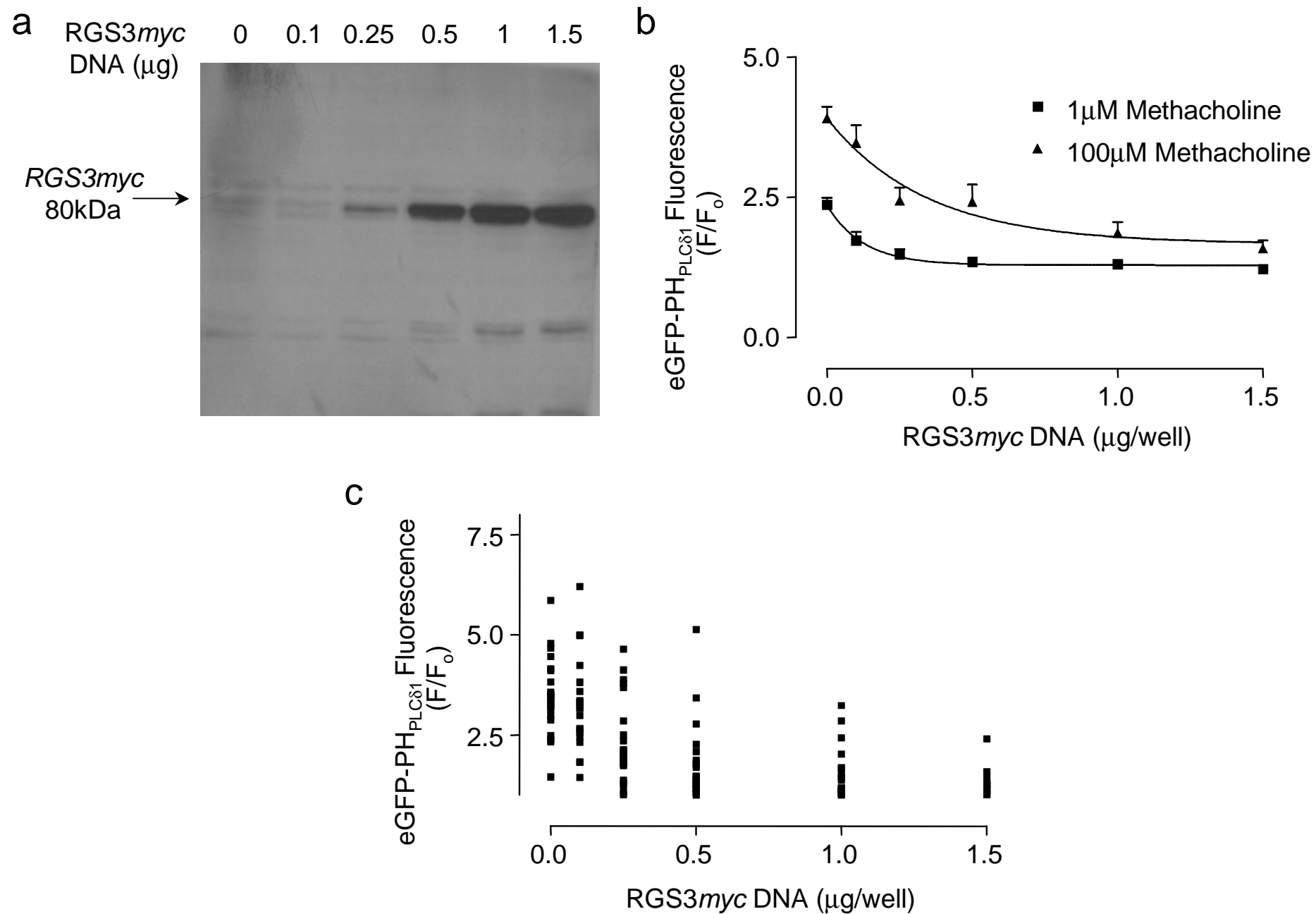


FIG. 5.

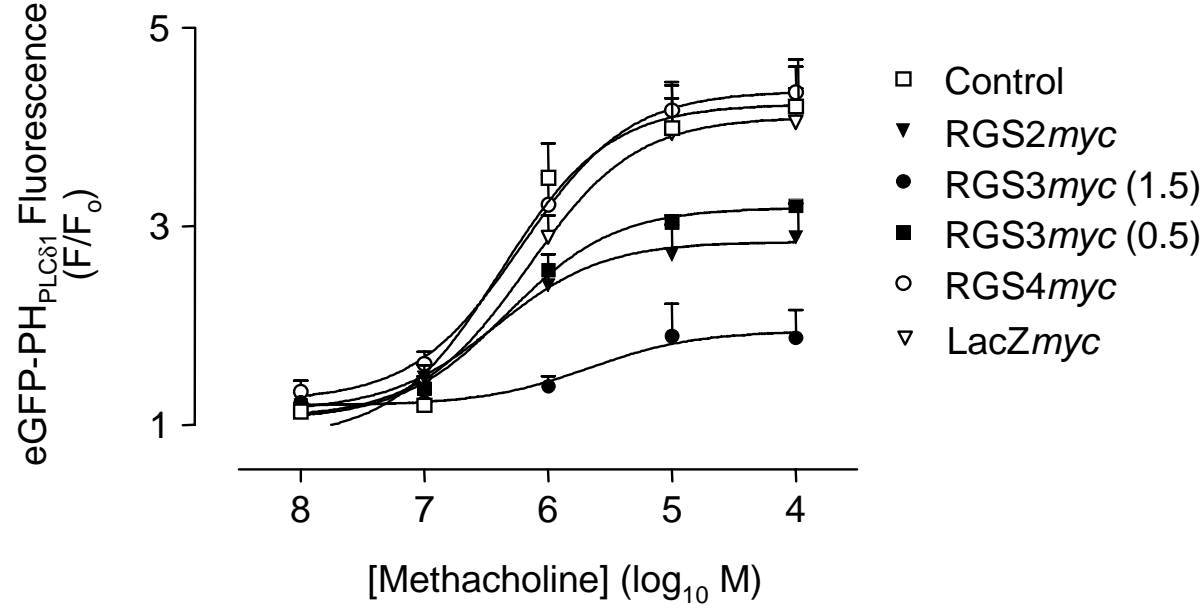


FIG. 6.

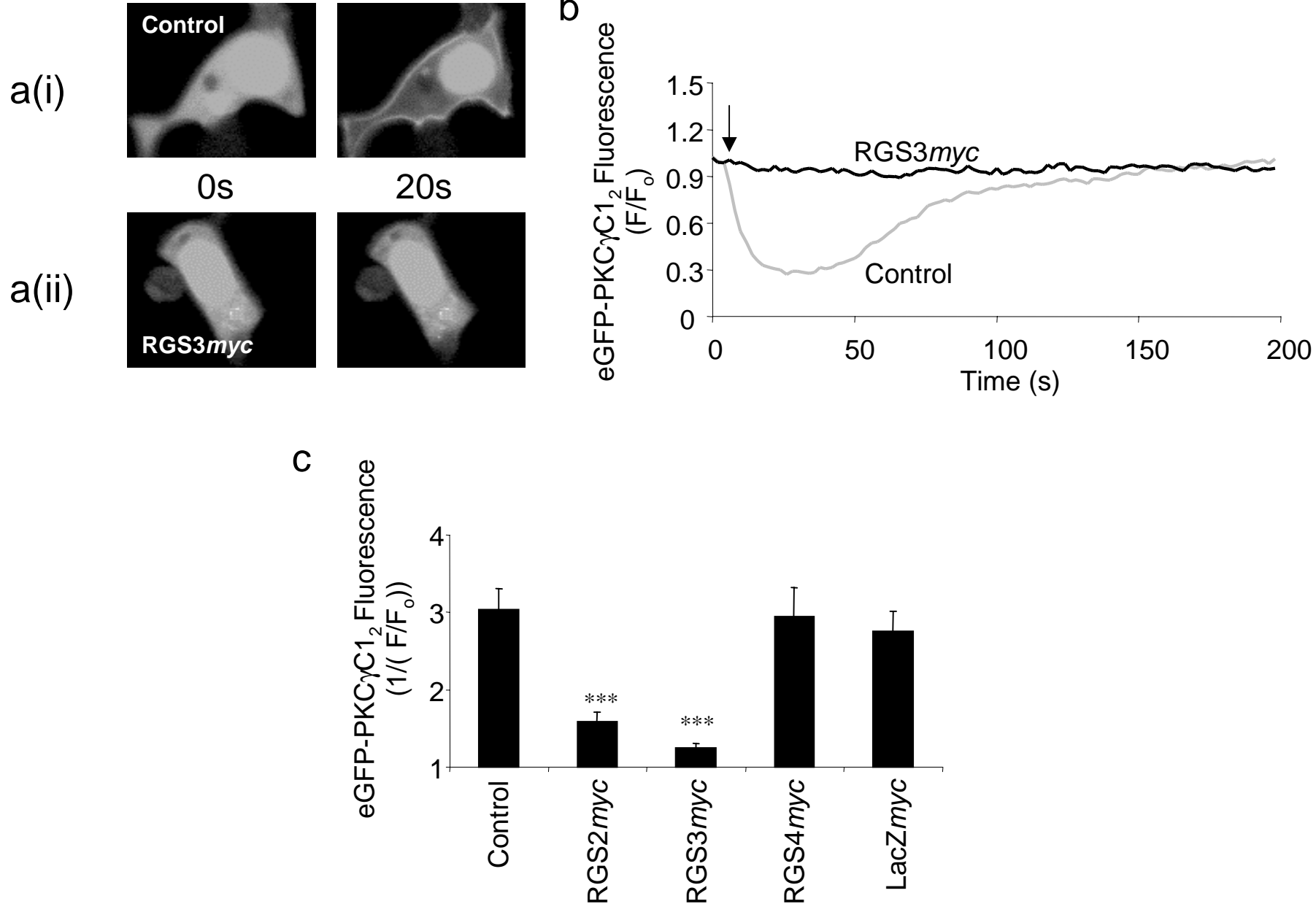
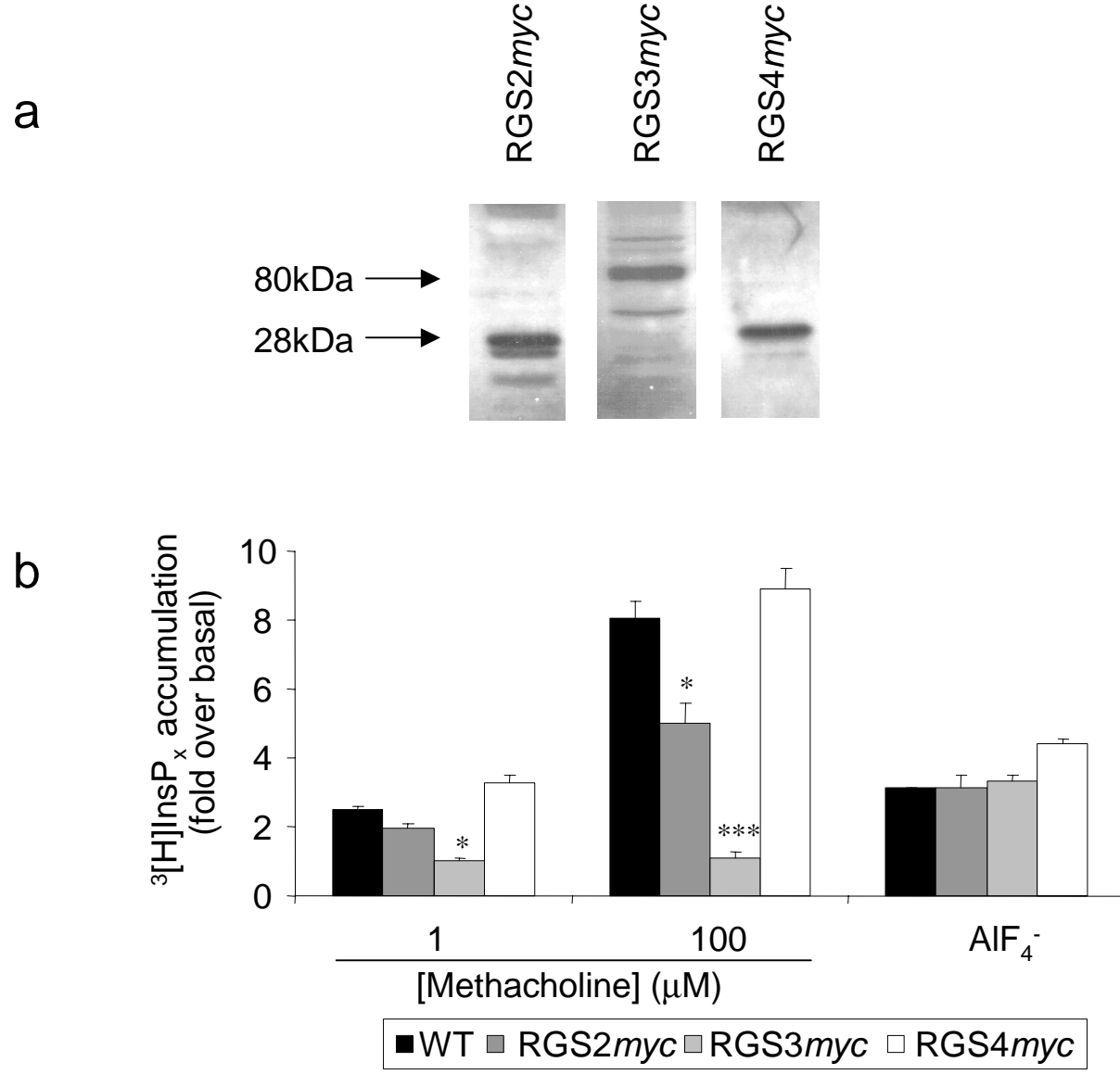


FIG. 7.



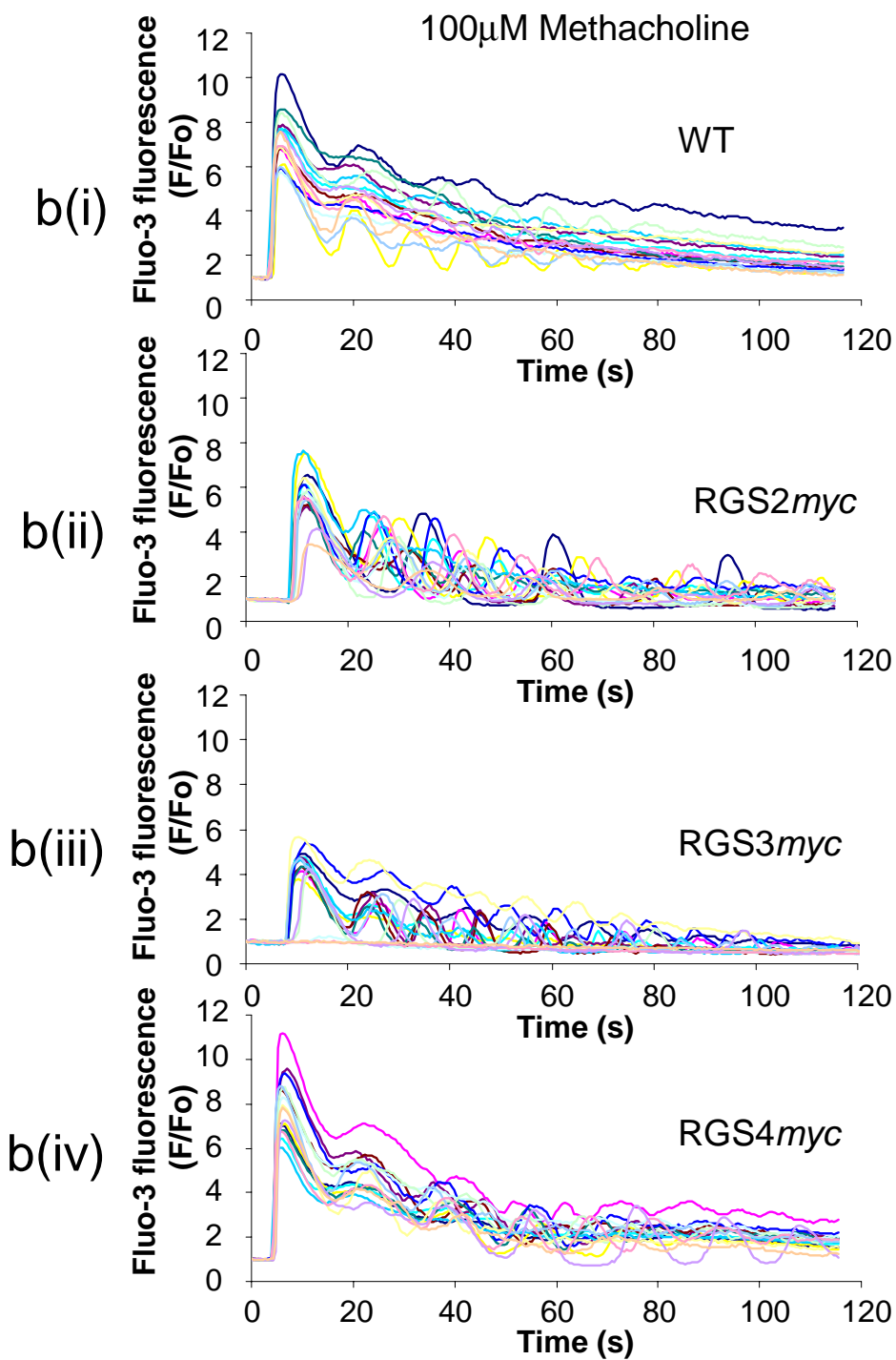
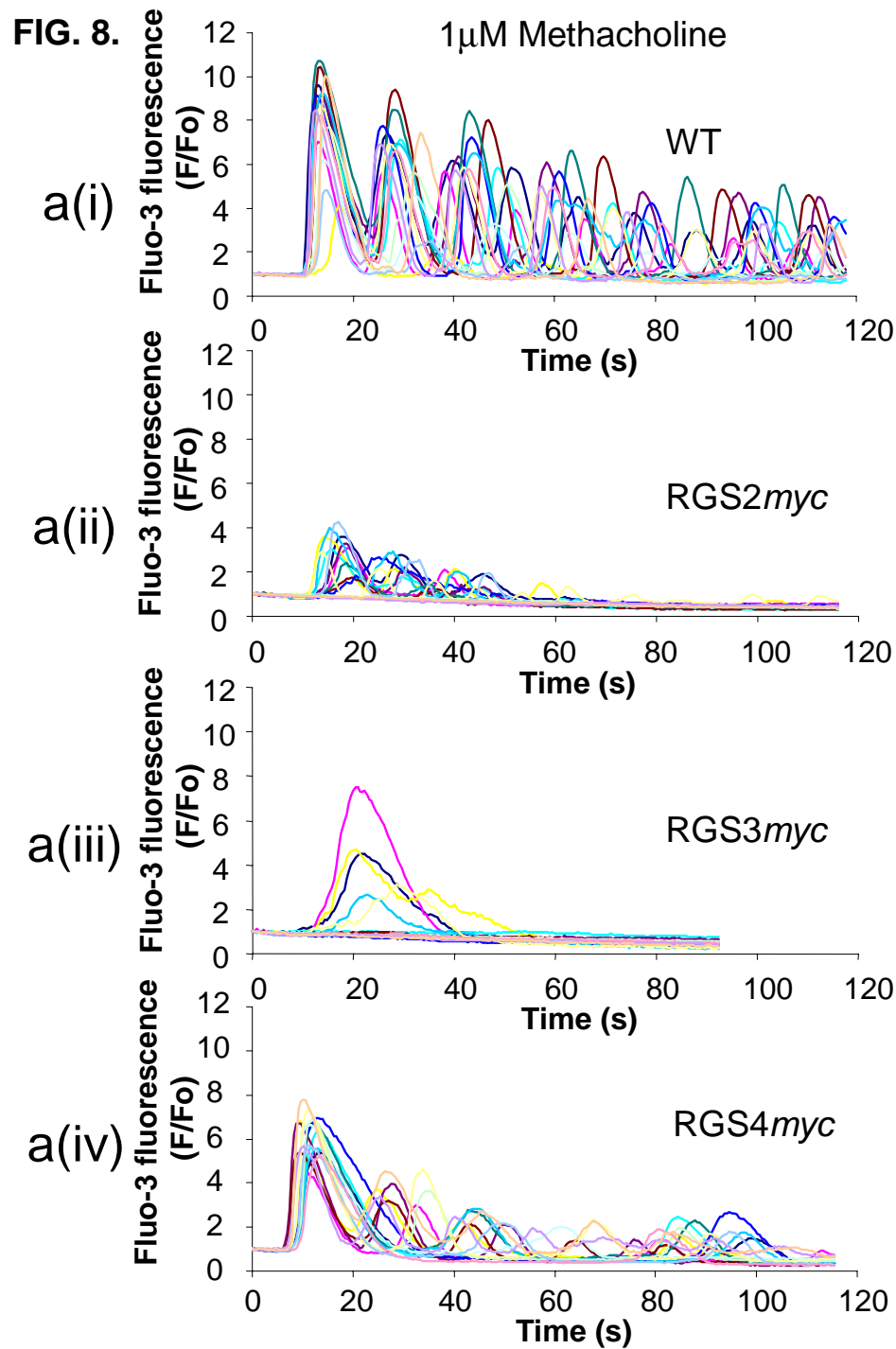


FIG. 9.

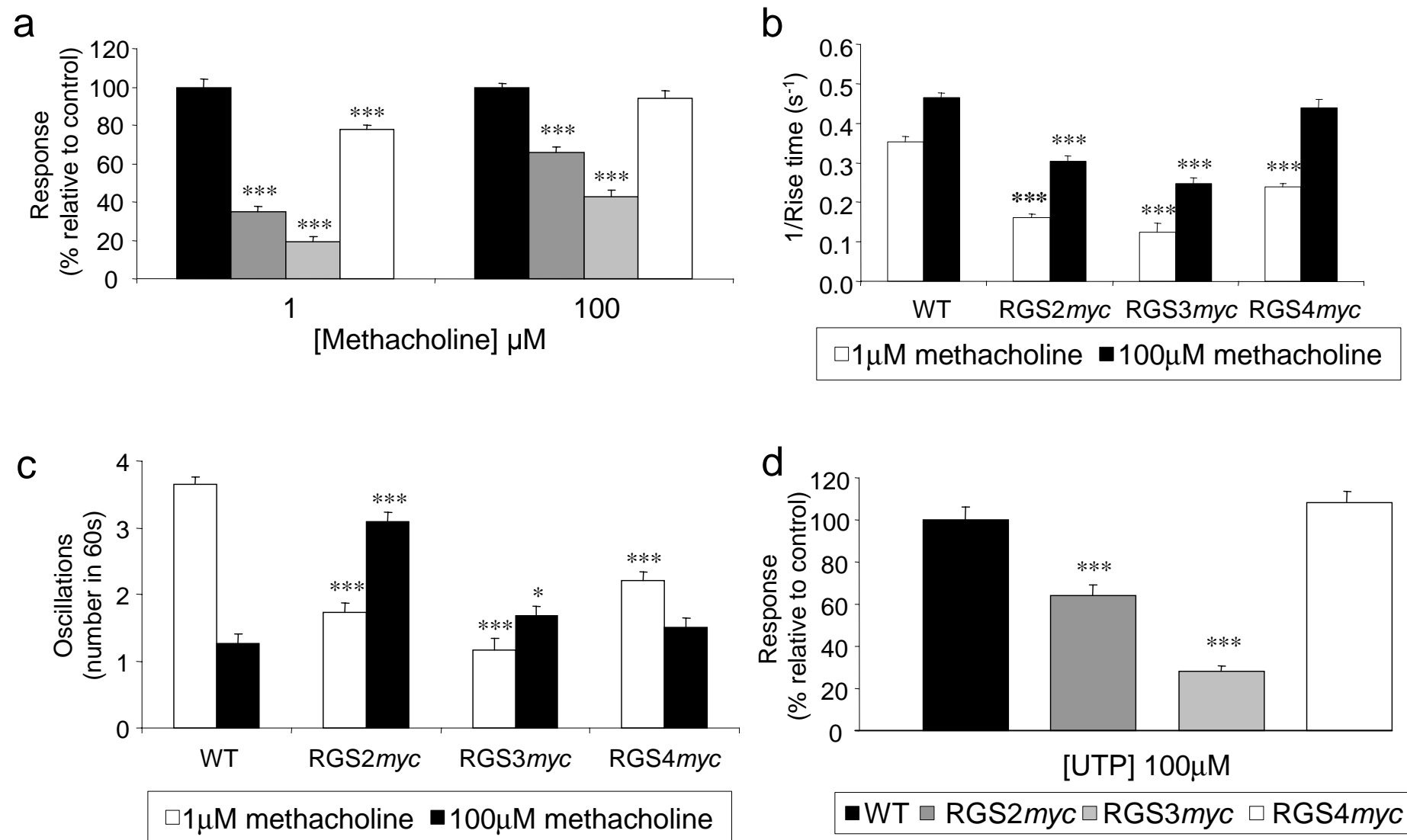


FIG. 10.

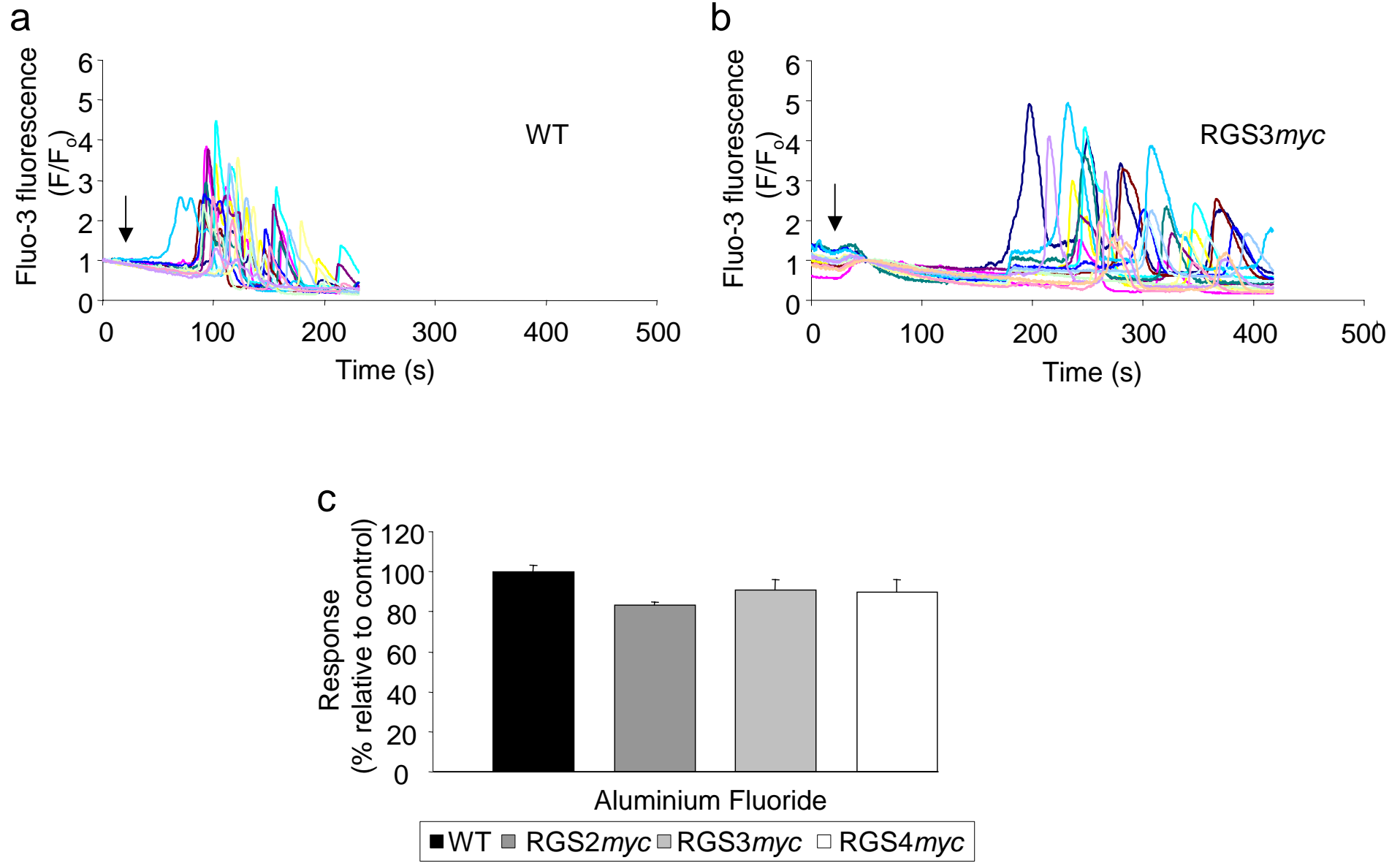


FIG. 11.

